Kavli Institute for the Physics and Mathematics of the Universe (IPMU),
APEC Seminar, November 6, 2019 – Kashiwa, Japan

Direct Multipixel Imaging of an exo-Earth with a Solar Gravitational Lens Telescope

Slava G. Turyshev

Jet Propulsion Laboratory, California Institute of Technology
4800 Oak Grove Drive, Pasadena, CA 91009 USA

A nice family portrait…

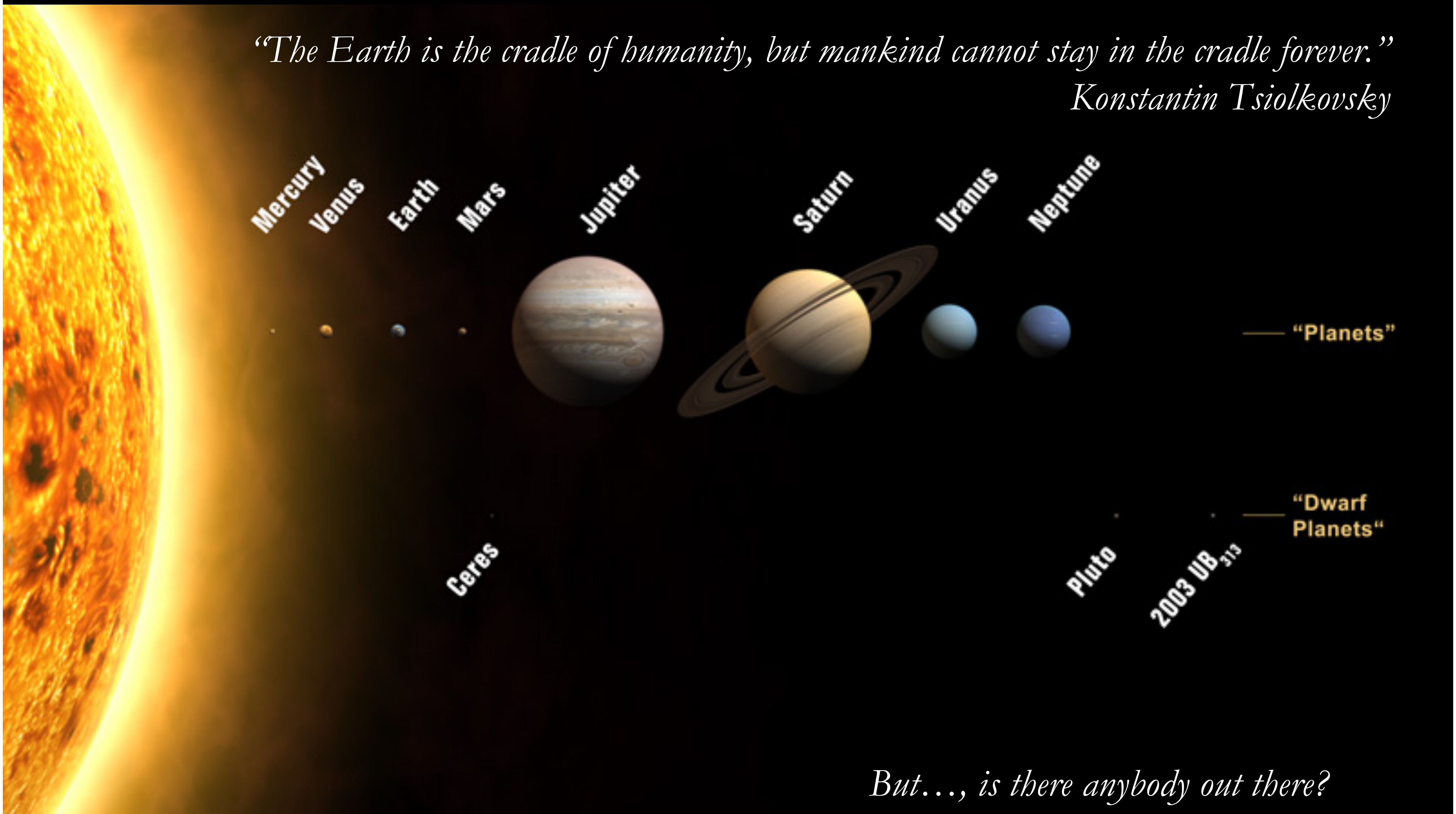

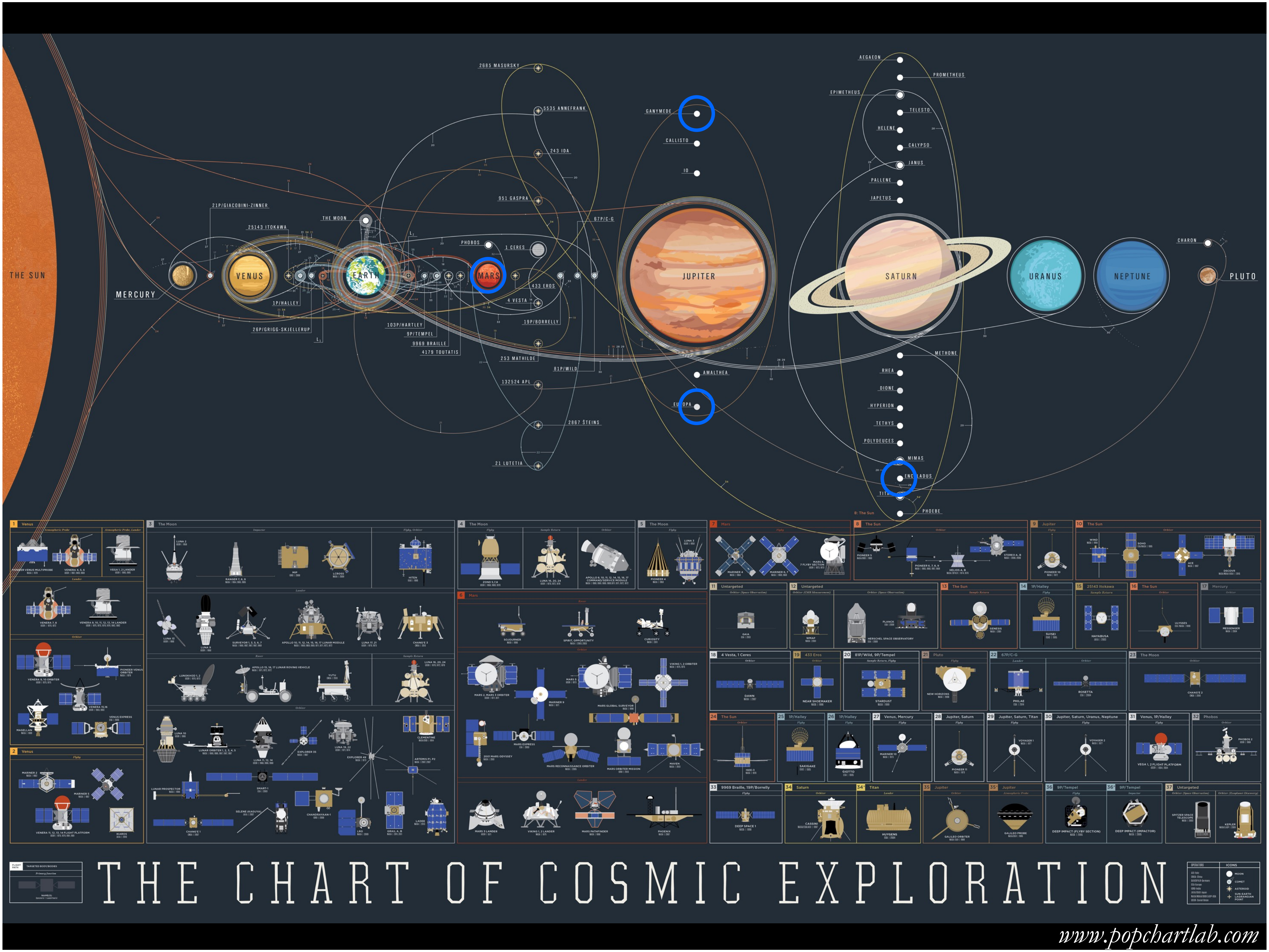
THE CHART OF COSMIC EXPLORATION
THE SUN
MERCURY
VENUS
EARTH
THE MOON
MARS
PHOBOS
1 CERES
JUPITER
GANYMEDE
CALLISTO
IO
AMALTHEA
EUROPA
SATURN
AEGAEON
PROMETHEUS
EPIMETHEUS
TELESTO
HELENE
CALYPSO
JANUS
PALLENE
IAPETUS
METHONE
RHEA
DIONE
HYPERION
TETHYS
POLYDEUCES
MIMAS
ENCELADUS
PHOEBE
URANUS
NEPTUNE
CHARON
PLUTO
2685 MASURSKY
5535 ANNEFRANK
243 IDA
951 GASPRA
67P/C-G
433 EROS
4 VESTA
19P/BORRELLY
253 MATHILDE
81P/WILD
132524 APL
2867 STEINS
21 LUTETIA
21P/GIACOBINI-ZINNER
25143 ITOKAWA
1P/HALLEY
26P/GRIGG-SKJELLERUP
103P/HARTLEY
9P/TEMPEL
9969 BRAILLE
4179 TOUTATIS
www.popchartlab.com

Solar system is not alone!

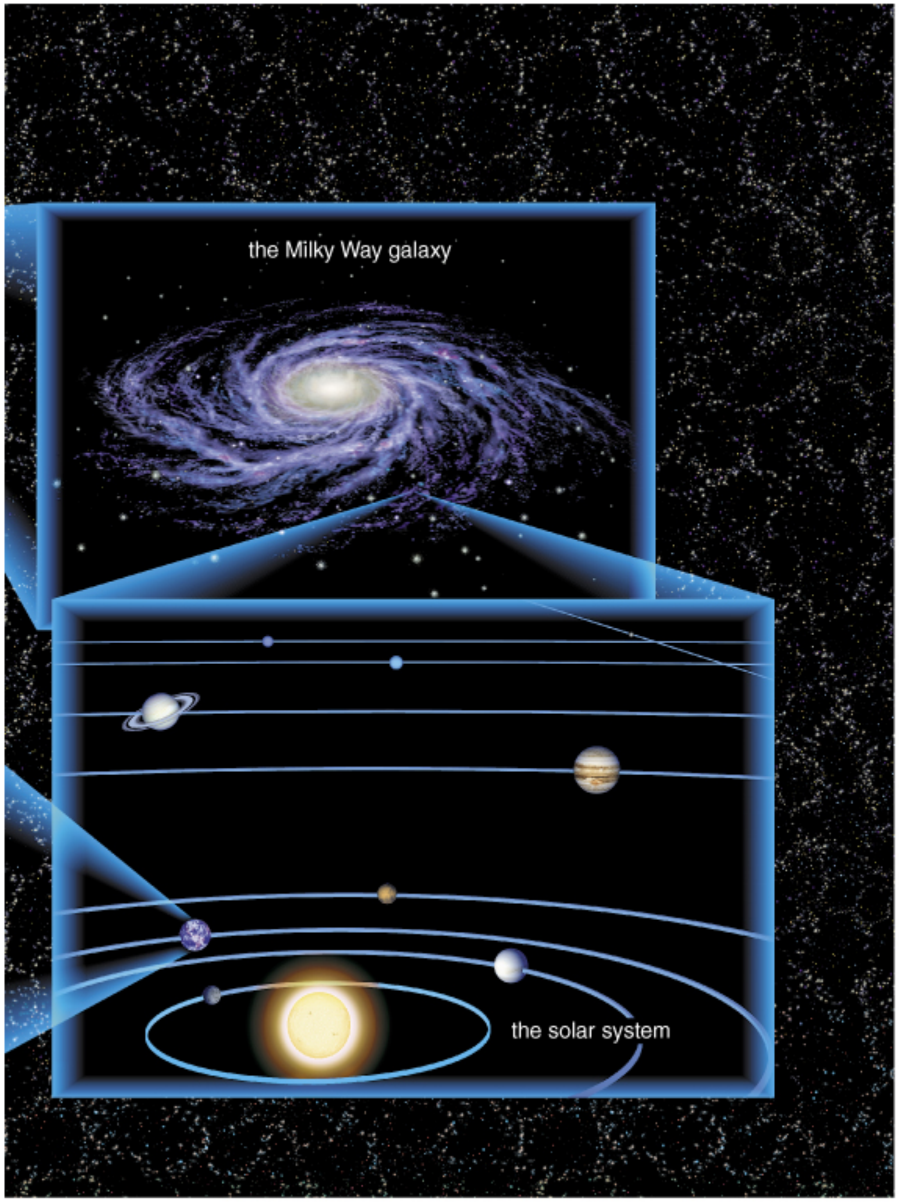

Current estimates:

- ~50% of stars have planets;
- ~100 billion stars in our Galaxy, and 1-10 planets per star;
- 50 billion to 5 trillion planets in our Galaxy (alone);
- There are ~10 new stars forming each year in our Galaxy…
- ~5 new planetary systems/year…
- ~5-50 new planets/year.

Exoplanet census (Oct 2019):

- 4,073 – confirmed;
- 4,495 – candidates;
- 3,028 – planetary systems;
- 161 – terrestrial.

Finding Earth 2.0 is matter of time...

– but what will we do once we find it?

https://exoplanets.nasa.gov/

Our Stellar Neighborhood within 100 ly

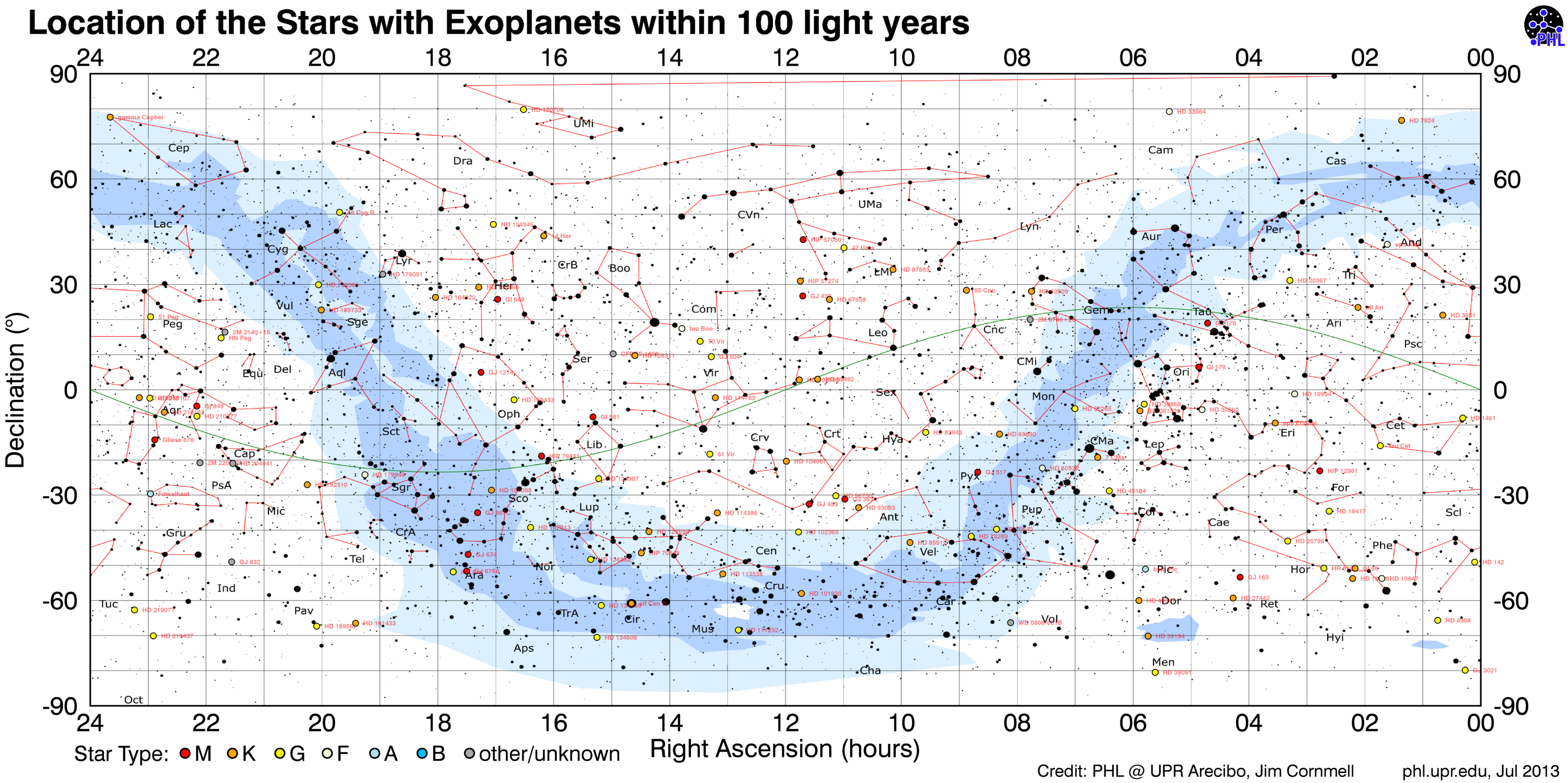

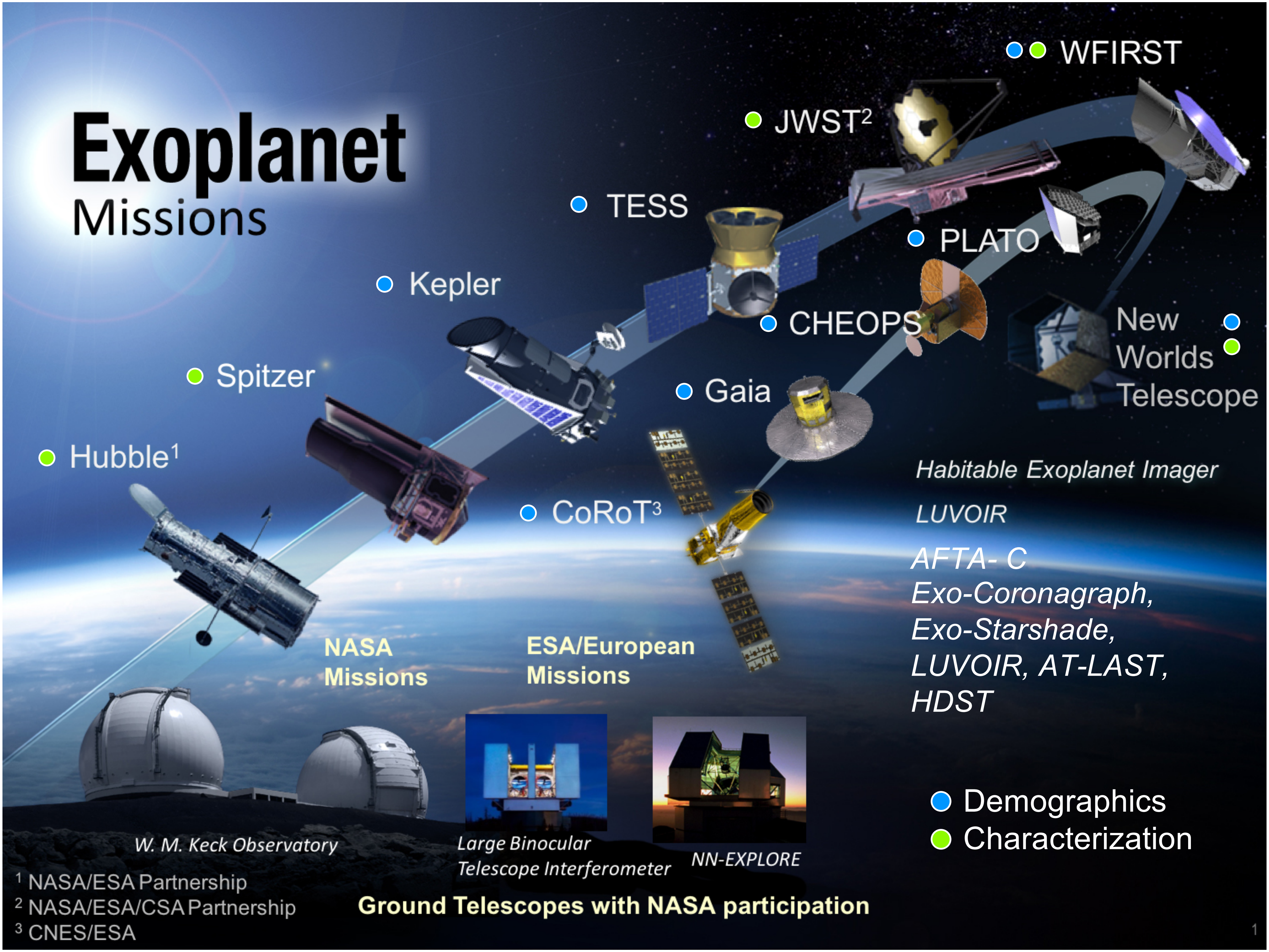
Exoplanet
Missions
WFIRST
JWST2
TESS
PLATO
Kepler
CHEOPS
New
Worlds
Telescope
Spitzer
Gaia
Hubble1
Habitable Exoplanet Imager
CoRoT3
LUVOIR
AFTA- C
Exo-Coronagraph,
Exo-Starshade,
LUVOIR, AT-LAST,
HDST
NASA
Missions
ESA/European
Missions
Demographics
Characterization
W. M. Keck Observatory
Large Binocular
Telescope Interferometer
NN-EXPLORE
1 NASA/ESA Partnership
2 NASA/ESA/CSA Partnership
3 CNES/ESA
Ground Telescopes with NASA participation
1

The size does matter…

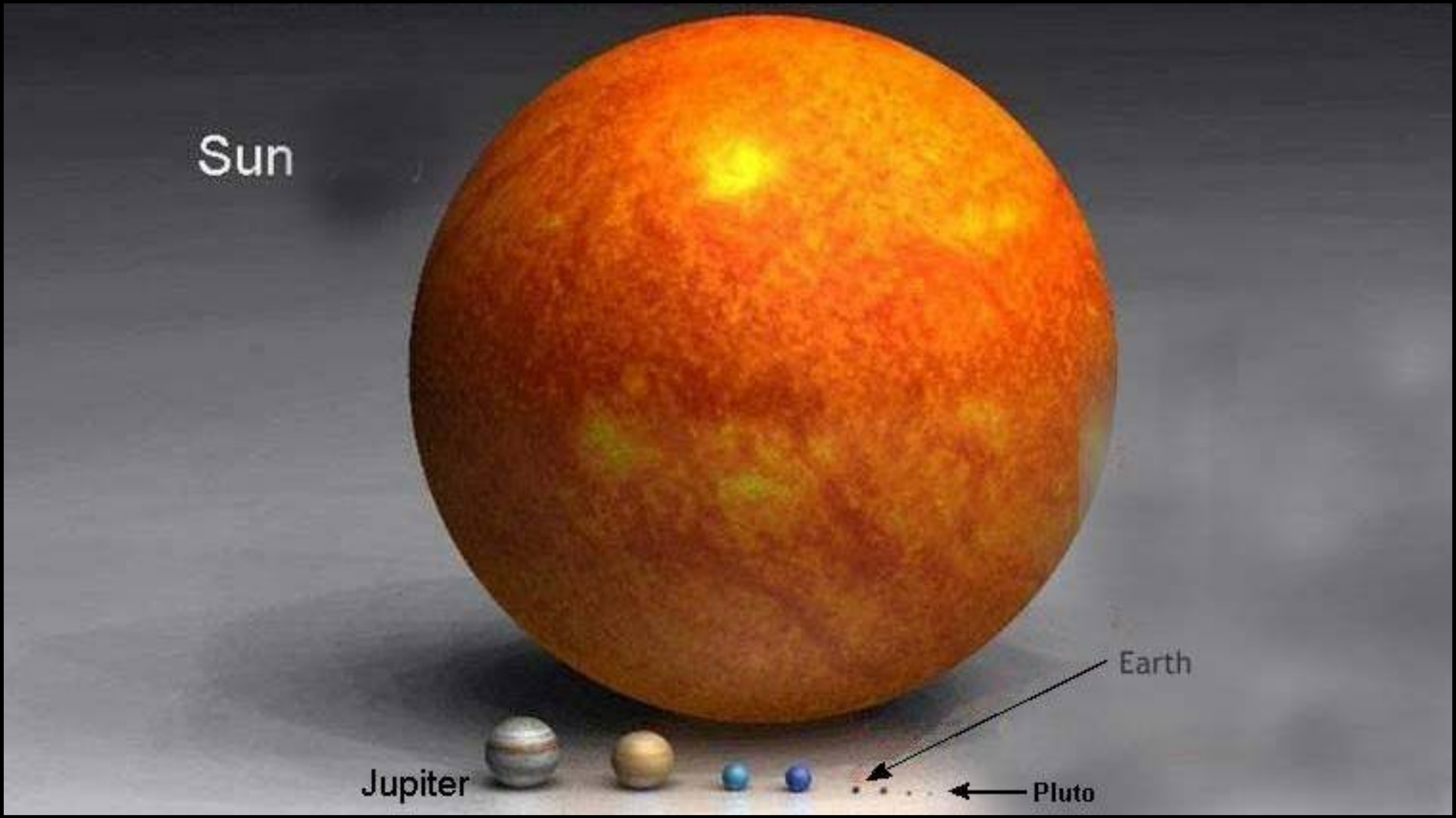

…and so does the distance: *the tyranny of the diffraction limit…*

Our Challenge

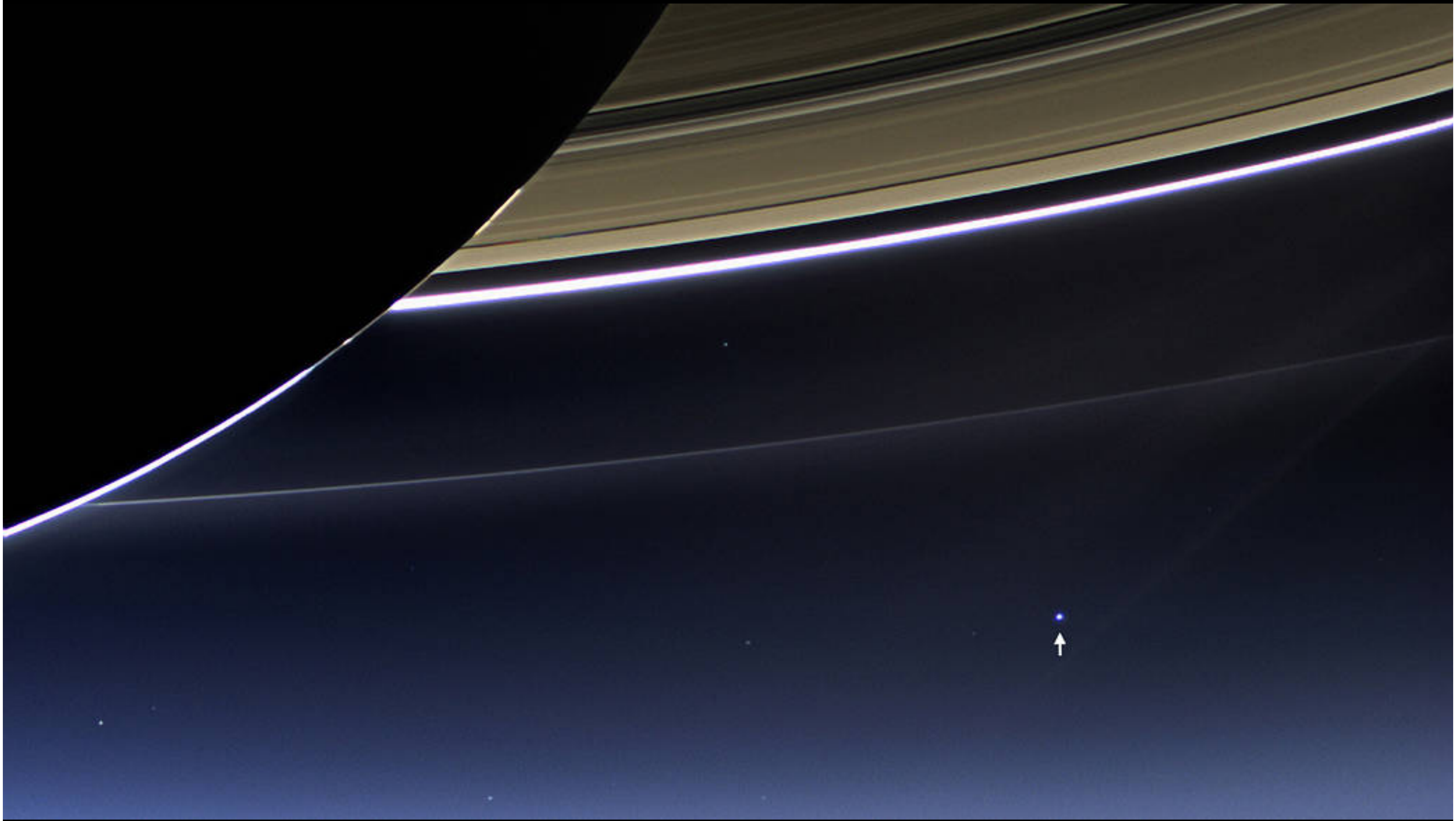

1-pixel direct image of an exo-Earth…

The tyranny of the diffraction limit: To make a 1-pixel image of an exo-Earth at 100 light years, one needs a telescope with a diameter of ~90 km…

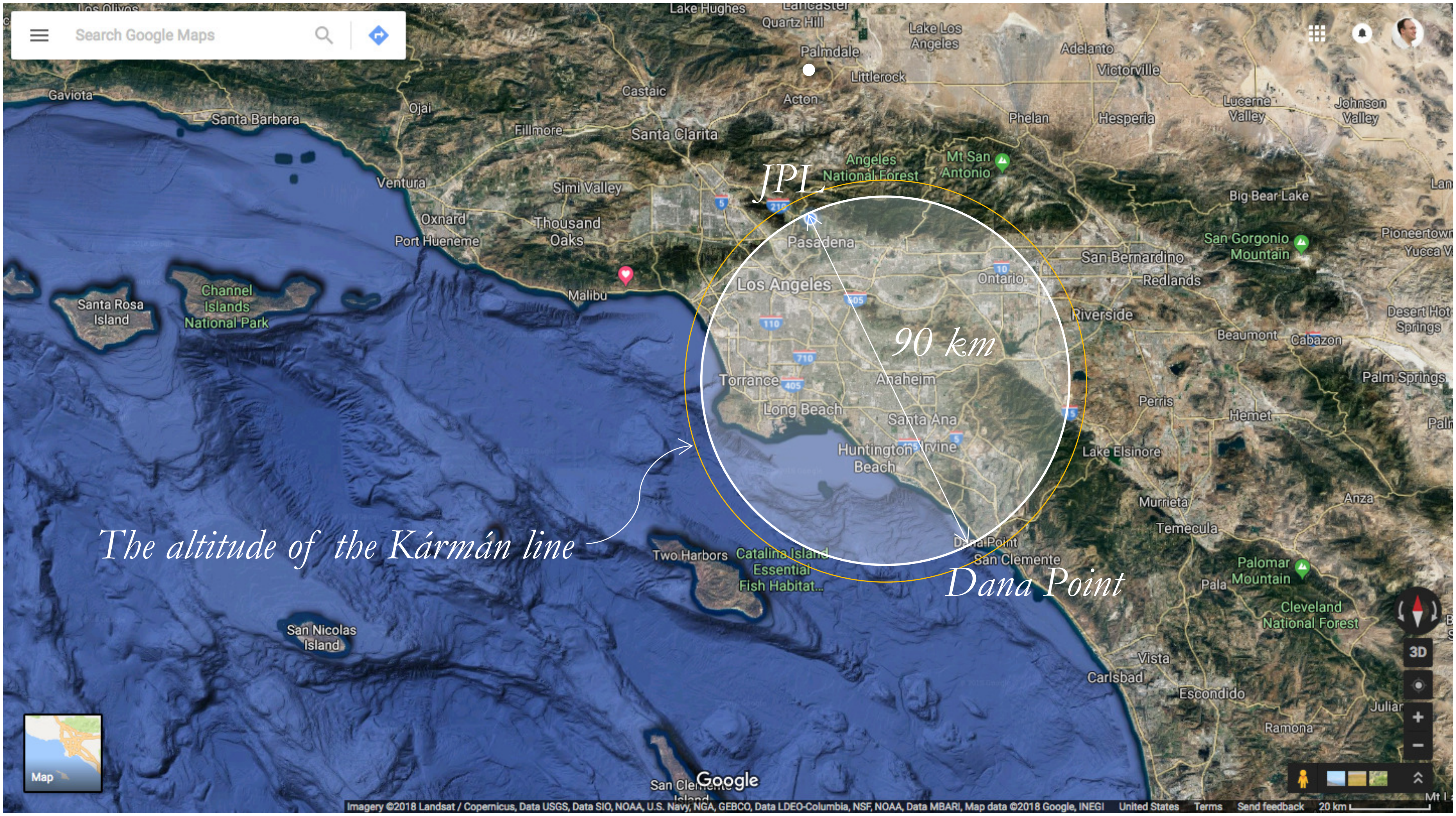

A (10k×10k)-pixels image of our Earth

This 2002 Blue Marble image features land surfaces, clouds, topography, and city lights at a maximal resolution of 1 km per pixel.

Composed from 4 months data from NASA's Terra satellite by R.Simmon, R.Stöckli.

1,000-pixel direct image of an exo-Earth…

The tyranny of the diffraction limit: To make a 1,000-pixel image of an exo-Earth at 100 light years, a telescope with a diameter of ~90,000 km is needed…

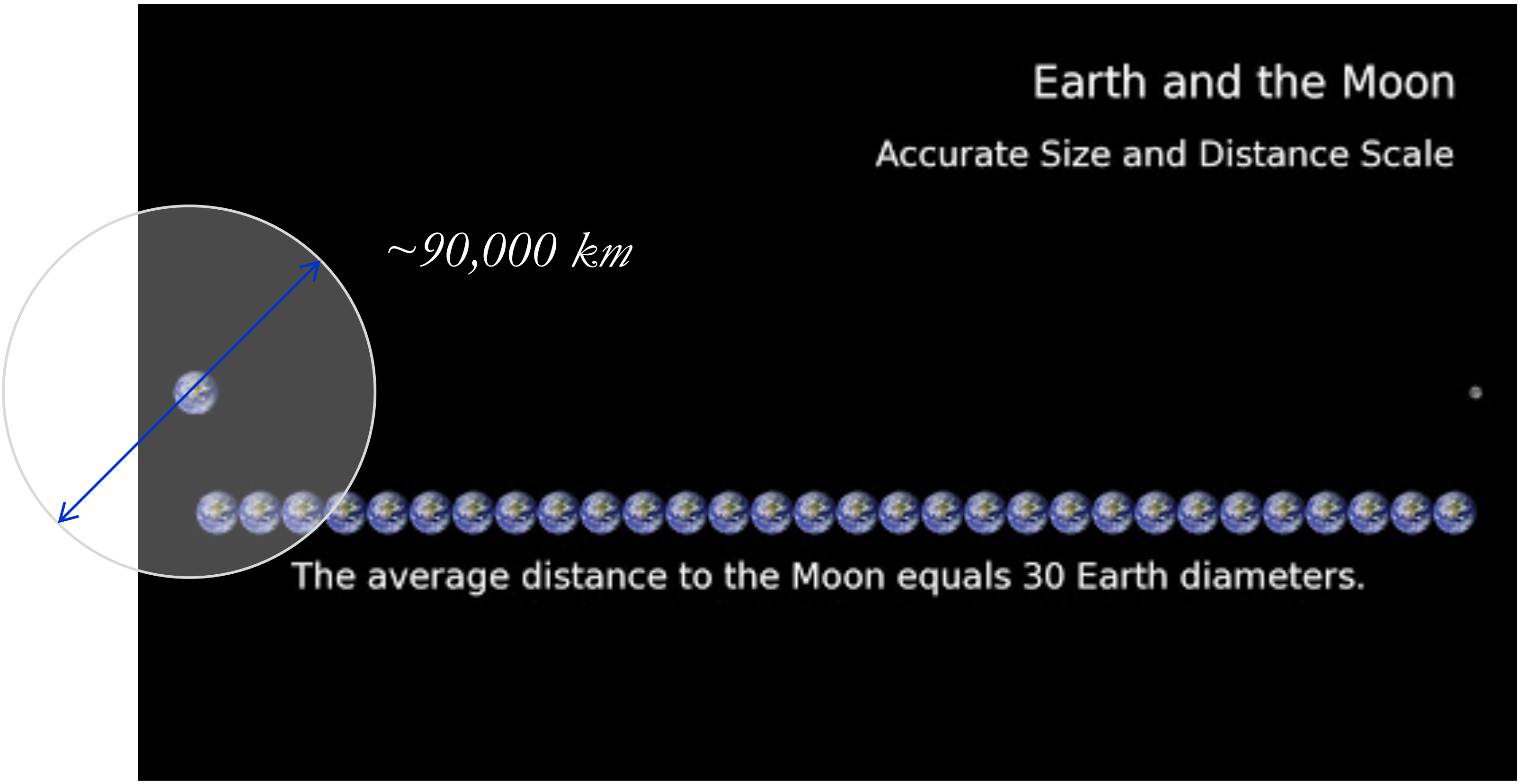

Diameter of 90,000 km is ~7 diameters of the Earth

Largest telescopes to date…

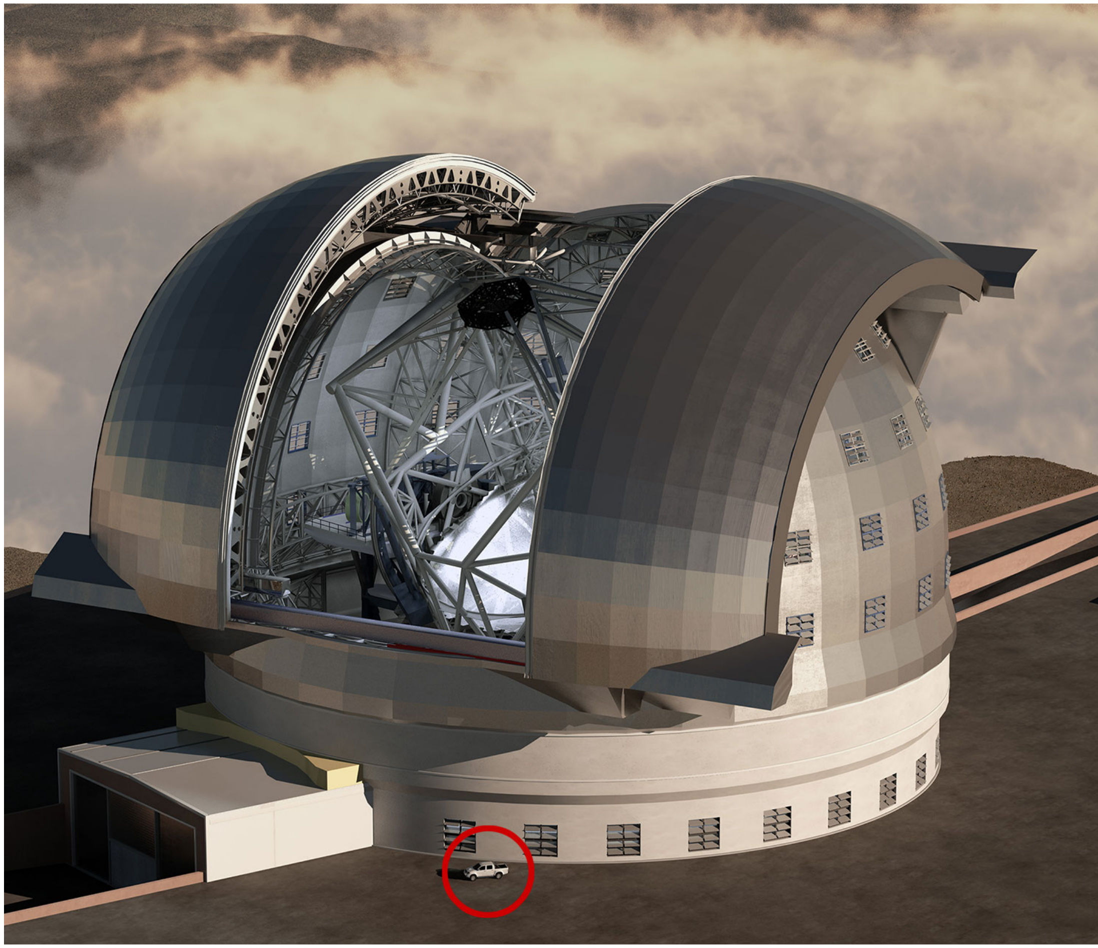

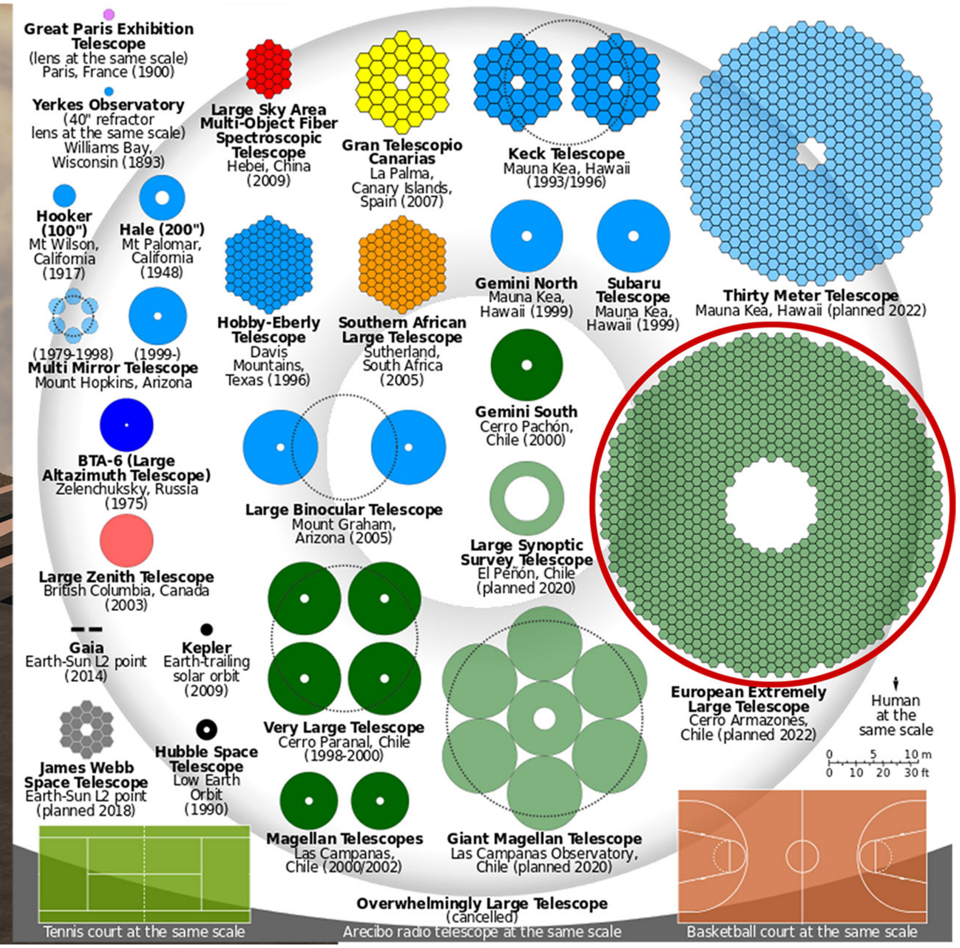

European Extremely Large Telescope
39 meters, Chile (est. 2022)

The largest telescopes for the last 125 years to date, both on the ground and in space

Largest telescopes in space

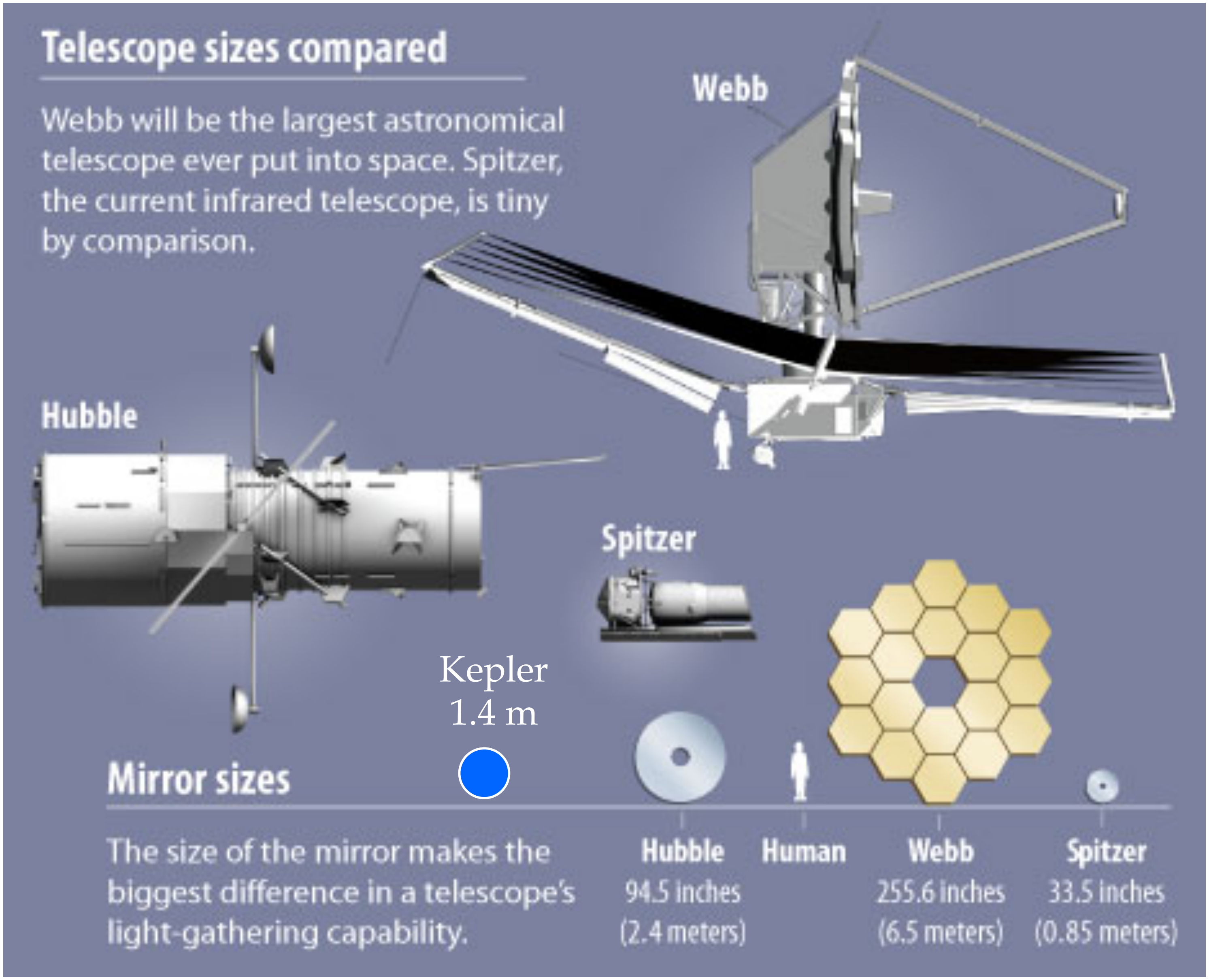

The Solar Gravitational Lens (KISS study, 2015)

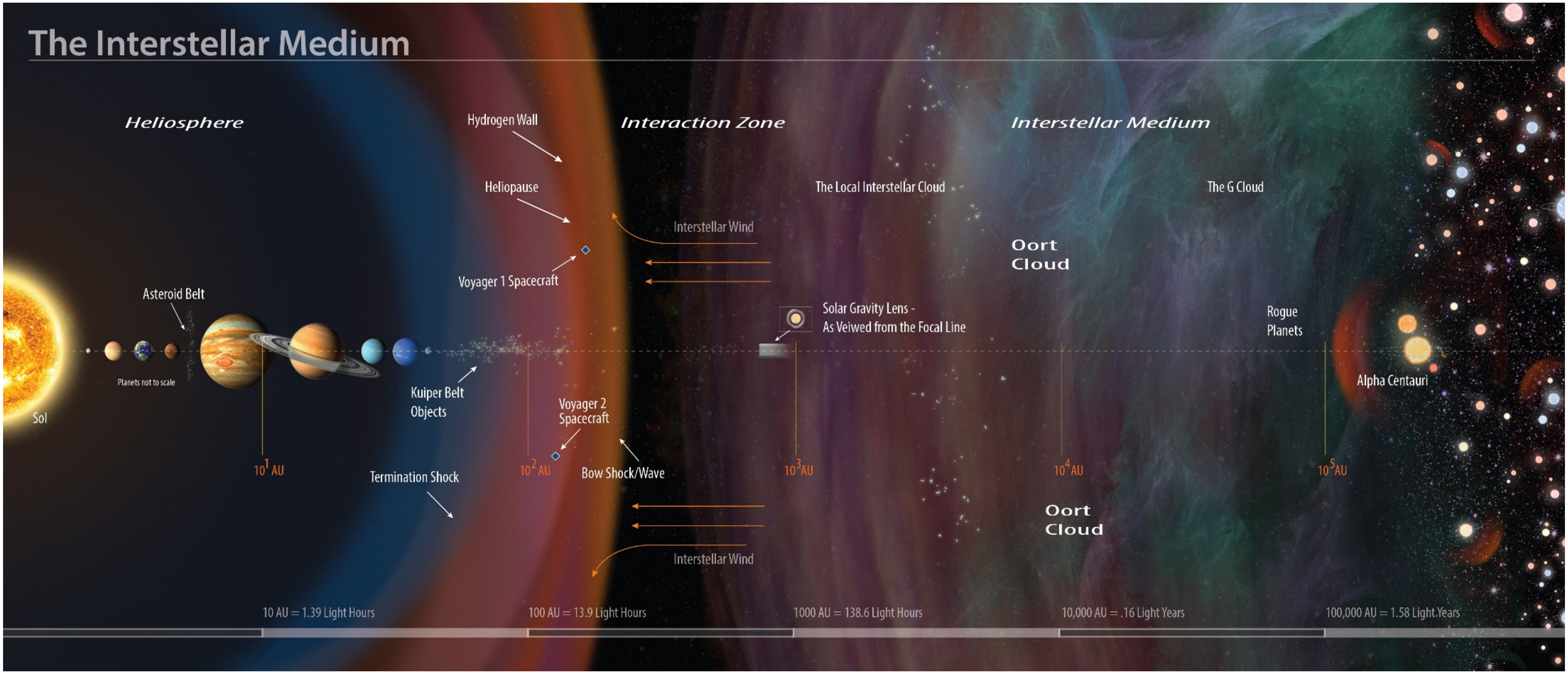

Earth-like Source

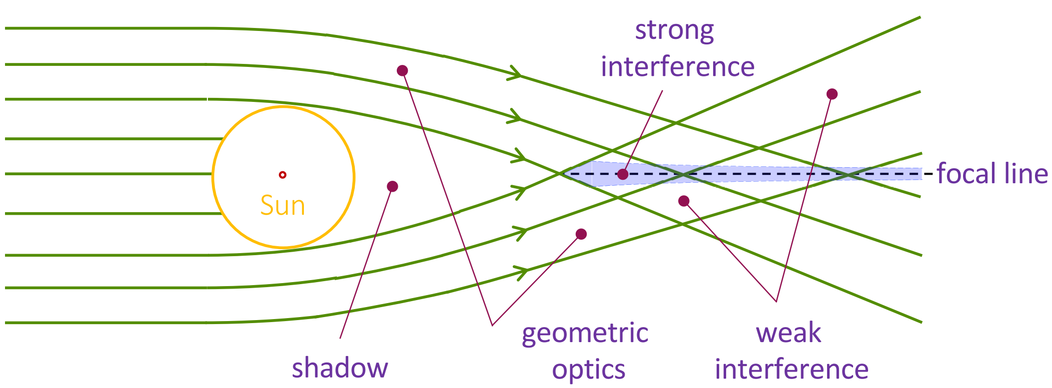

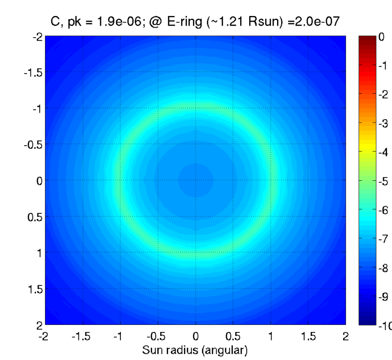

Image

The image within the Einstein ring

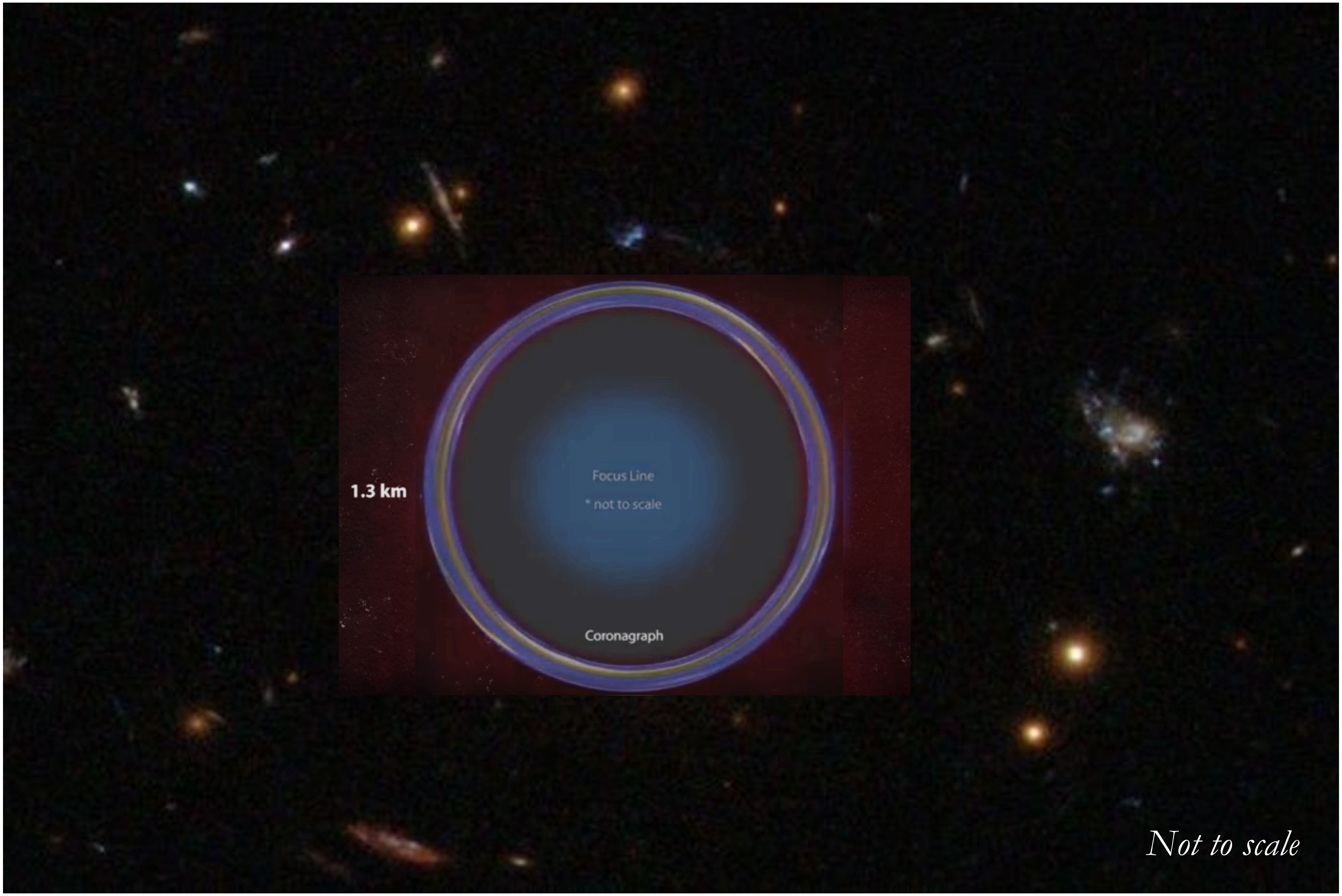

Credit: ESA, Hubble & NASA Wikimedia

Properties of the Solar Gravity Lens

$$\mu^0_{\mathtt{SGL}} = \frac{4\pi^2}{1-e^{-4\pi^2 r_g/\lambda}}\frac{r_g}{\lambda}\,J_0^2\Big(2\pi\frac{\rho}{\lambda}\sqrt{\frac{2r_g}{\overline{z}}}\Big) = 1.12\times 10^{11}\,J_0^2\Big(48.98\Big(\frac{\rho}{1\,\mathrm{m}}\Big)\Big(\frac{1\,\mu\mathrm{m}}{\lambda}\Big)\Big(\frac{650\,\mathrm{AU}}{\overline{z}}\Big)^{\frac{1}{2}}\Big)$$

- Important features of the SGL (for λ = 1 μm):
  - Major brightness amplification: a factor of 10^{11} (on the optical axis);
  - High angular resolution: ~0.5 nano-arcsec. A 1-m telescope at the SGL collects light from a ~(10km × 10km) spot on the surface of the planet, bringing this light to one 1-m size pixel in the image plane of the SGL;
  - Extremely narrow “pencil” beam: entire image of an exo-Earth (~13,000 km) at 100 l.y. is included within a cylinder with a diameter of ~1.3 km.

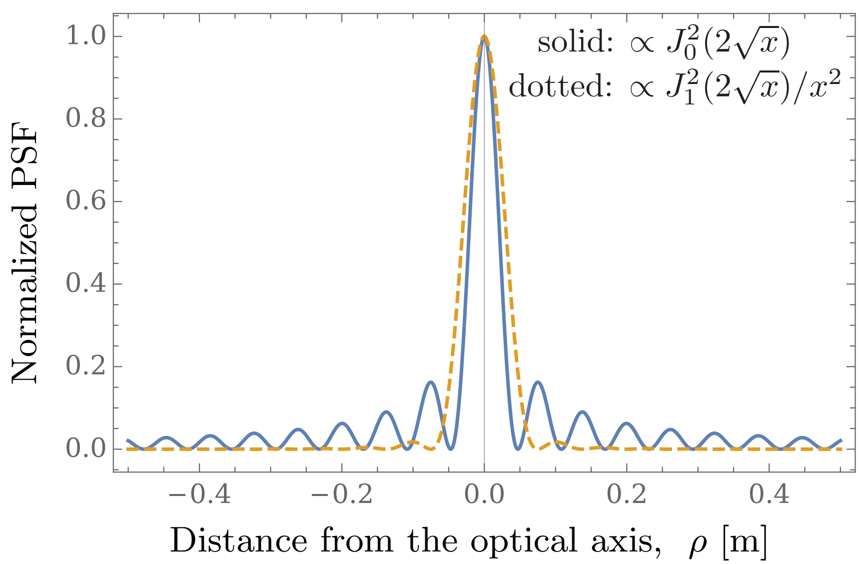

Turyshev & Toth, Phys. Rev. D 96, 024008 (2017)

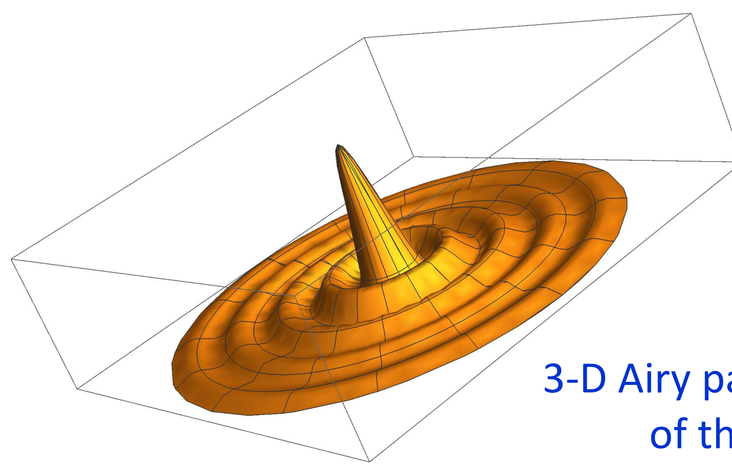

3-D Airy pattern of the SGL

Mission to the Gravity Lens of the Sun

Eshleman V.R., Science **205**, 1133 (1979)

Gravitational Lens of the Sun: Its Potential for Observations and Communications over Interstellar Distances

Abstract. *The gravitational field of the sun acts as a spherical lens to magnify the intensity of radiation from a distant source along a semi-infinite focal line. A spacecraft anywhere on that line in principle could observe, eavesdrop, and communicate over interstellar distances, using equipment comparable in size and power with what is now used for interplanetary distances. If one neglects coronal effects, the maximum magnification factor for coherent radiation is inversely proportional to the wavelength, being 100 million at 1 millimeter. The principal difficulties are that the nearest point on the focal half-line is about 550 times the sun-earth distance, separate spacecraft would be needed to work with each stellar system of interest, and the solar corona would severely limit the intensity of coherent radiation while also restricting operations to relatively short wavelengths.*

About 40 years ago, Einstein (*1*) published a short note in *Science* on the focusing of starlight by the gravitational field of another star. He emphasized the improbability of observing this phenomenon by the chance alignment of two stars and the earth. From concepts based on current technology and trends, however, it appears that gravitational focusing of electromagnetic radiation might be employed, by design, for highly directional observations and communications over interstellar distances.

In such use, the gravitational field of the sun could play several roles. First, it might be used to reduce fuel and time re- … $1 + \nu$, where the refractivity $\nu = g/r$ at radius r. A ray is deflected through the angle $\alpha = 2g/a$, where a is the ray impact parameter and g is the gravitational radius ($g = 2Gm/c^2$, where G is the gravitational constant, m is the mass of the central body, and c is the speed of light). It is assumed throughout that $\alpha << 1$. An observer at position z behind the lens and x from the center line, as illustrated, would see an energy density lessened by defocusing in the plane of propagation, but increased by focusing due to the curved limb normal to this plane. The relative single-ray intensity $I = F_h^2 F_v^2$, where in ray optics $F_h^2 =$ … nel scales along the circumference of a circle at the ray-impact radius. Using also the wave number $k = 2\pi/\lambda$, the maximum intensification of the coherent signal is simply

$$I_{max} = 2\pi kg \tag{2}$$

As an approximation, let the focal "spot" radius x_s be the value of x where I falls to $I_{max}/4$, so that $x_s = (2/\pi k)(z/2g)^{1/2}$. Thus the angular resolution for distinguishing two adjacent coherent sources by a corresponding change in intensity is x_s/z radians. (The first null off the center line is at $x = \pi^2 x_s/2$, and the first sidelobe is twice this distance with intensity I_{max}/π^2.) The periapsis or minimum radius of the ray relative to the center of mass is $a - g$, or essentially a, and this must be greater than r_0, the physical radius of the spherical mass. Thus $\alpha_{max} = 2g/r_0$ and the focal line begins at $z_{min} = r_0^2/2g$.

Now consider the focusing at $z > z_{min}$ of incoherent radiation from a uniformly bright, circular, extended source of radius r_p and distance $z_p >> z$. This is the problem considered by Einstein (*1*) and more completely by others, notably Liebes (*4*). The gain factor A of the gravitational lens for the intensity observed from the two individual image com-

Optical wavelengths magnification ~10^{11}

Kraus J.D., Radio Astronomy, Cygnus-Quasar Books, Powell, Ohio, 6-115 (1986)

Maccone C., many papers, 1999-present

Turyshev & Andersson, MNRAS **341**, 577 (2003)

Original gravity lens derivation (Einstein c.1911)

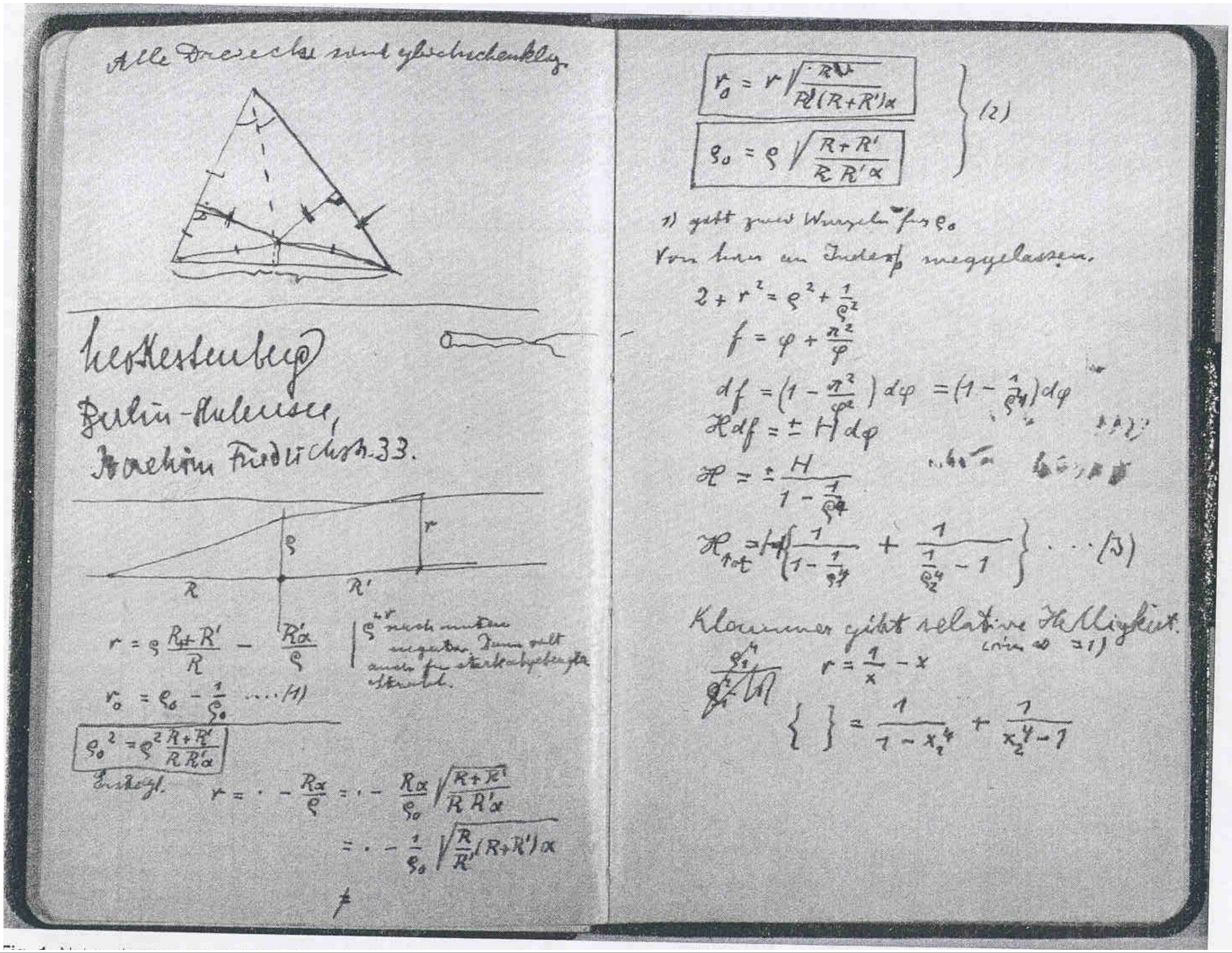

Precision alignment between a Lens and the Earth is very unlikely…

Gravitational deflection of light before GR

$$\alpha_{\texttt{Newton}}(b) = \frac{2GM_\odot}{c^2 b} = 0.877\left(\frac{\mathcal{R}_\odot}{b}\right)\ \mathrm{arcsec}$$

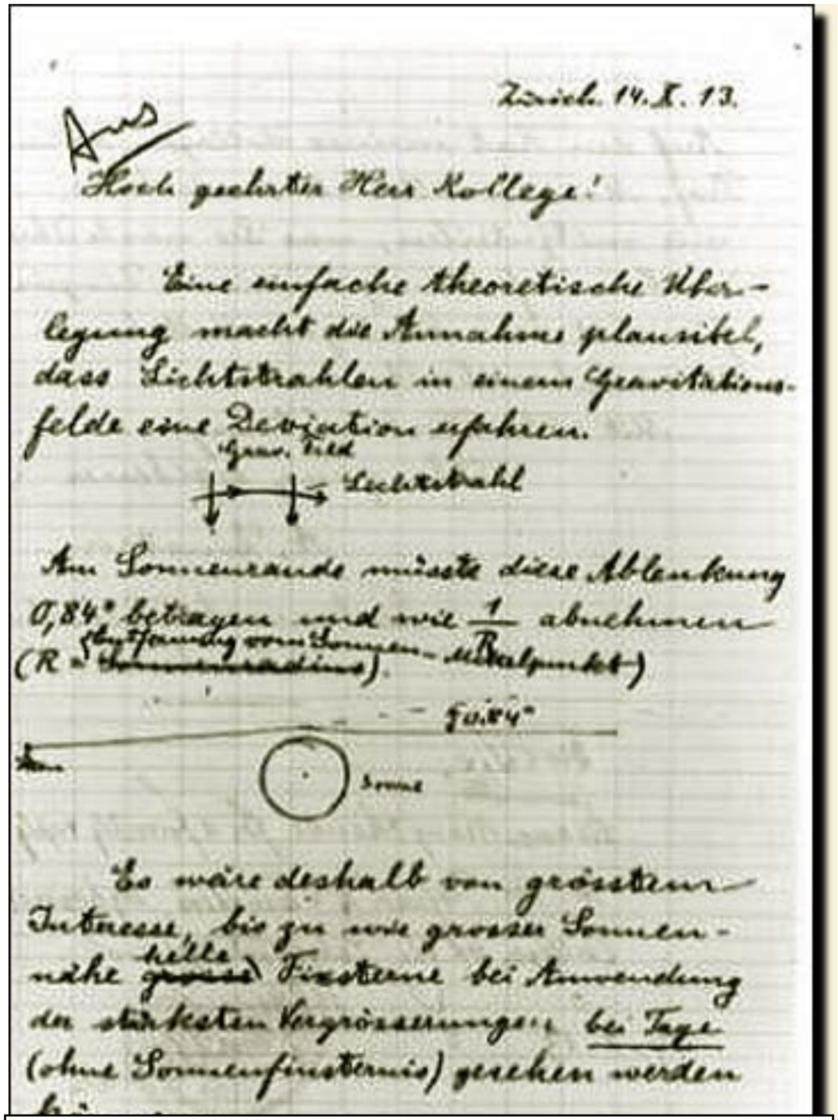
Zürich. 14. X. 13.

Ans

Hoch geehrter Herr Kollege!

Eine einfache theoretische Überlegung macht die Annahme plausibel, dass Lichtstrahlen in einem Gravitationsfelde eine Deviation erfahren.

Grav. feld

Lichtstrahl

Am Sonnenrande müsste diese Ablenkung 0,84" betragen und wie $\frac{1}{R}$ abnehmen (R = ~~Sonnenradius~~ Abstand vom Sonnen-Mittelpunkt).

= 0.84"

Sonne

Es wäre deshalb von grösstem Interesse, bis zu wie grosser Sonnennähe ~~grosse~~ helle Fixsterne bei Anwendung der stärksten Vergrösserungen bei Tage (ohne Sonnenfinsternis) gesehen werden

The Huntington Library, Pasadena, CA


Albert Einstein
c.1913

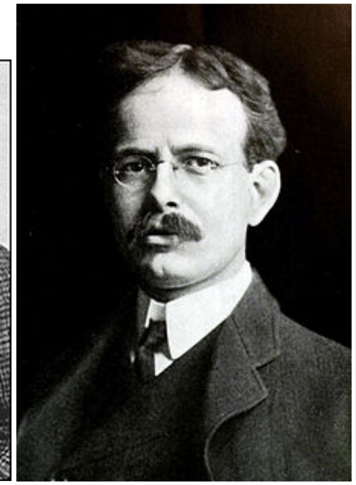
George Ellery Hale
(1868-1938)


Erwin Finlay-Freundlich
(1885-1964)

- In 1913 Einstein wrote to Hale:
  - "Is eclipse necessary to test this prediction?"
  - Hale replied: "Yes, an eclipse is necessary, as stars near the Sun would then be visible, and the bending of light from them would show up as an apparent displacement of the stars from their normal positions."
- In 1914, the first attempt - a German expedition
  - A German astronomer Finley-Freundlich led an expedition to test the Einstein's prediction during a total solar eclipse on Aug. 21, 1914 (in Russia);
  - However, the First World War (July 28, 1914) intervened, and no observations could be made.

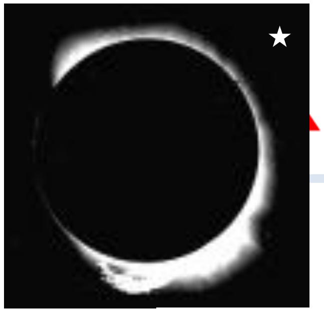

THE SOLAR GRAVITATIONAL LENS

The First Test of General Theory of Relativity

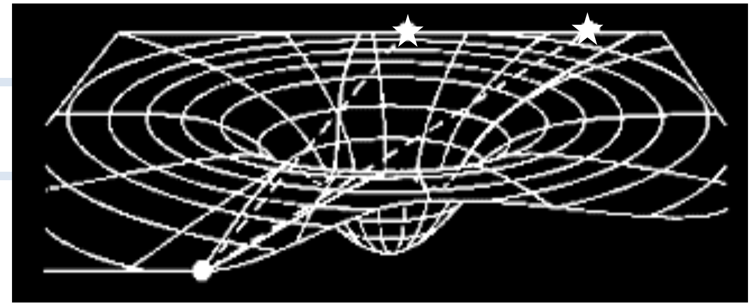

Gravitational Deflection of Light:

$$\alpha_{\rm GR}(b) = \frac{2(1+\gamma)GM_\odot}{c^2 b} \simeq 1.75\Big(\frac{1+\gamma}{2}\Big)\Big(\frac{\mathcal{R}_\odot}{b}\Big)\ \mathrm{arcsec}$$

Solar Eclipse 1919: possible outcomes

Deflection = 0;
Newton = 0.87 arcsec;
Einstein = 2 x Newton = 1.75 arcsec

037

einstein akademie vissenchaften
berlin

12/4 1923 Telegraphie des Deutschen Reichs.

[redacted] Antw S

Berlin, Haupt-Telegraphenamt

Antw S

[redacted] 5

lickobservaory calif 129/12 50 1r 19/16.- vesternunion

three pairs australia tahiti eclipse plates measured by campb
trumpler sixty two to eighty four stars each five of six
measurements completely calculated give einstein deflection
between one point fifty nine and one point eighty six seconds
arc mean value one point seventy four seconds = campbell .+

Campbell's telegram to Einstein, 1923

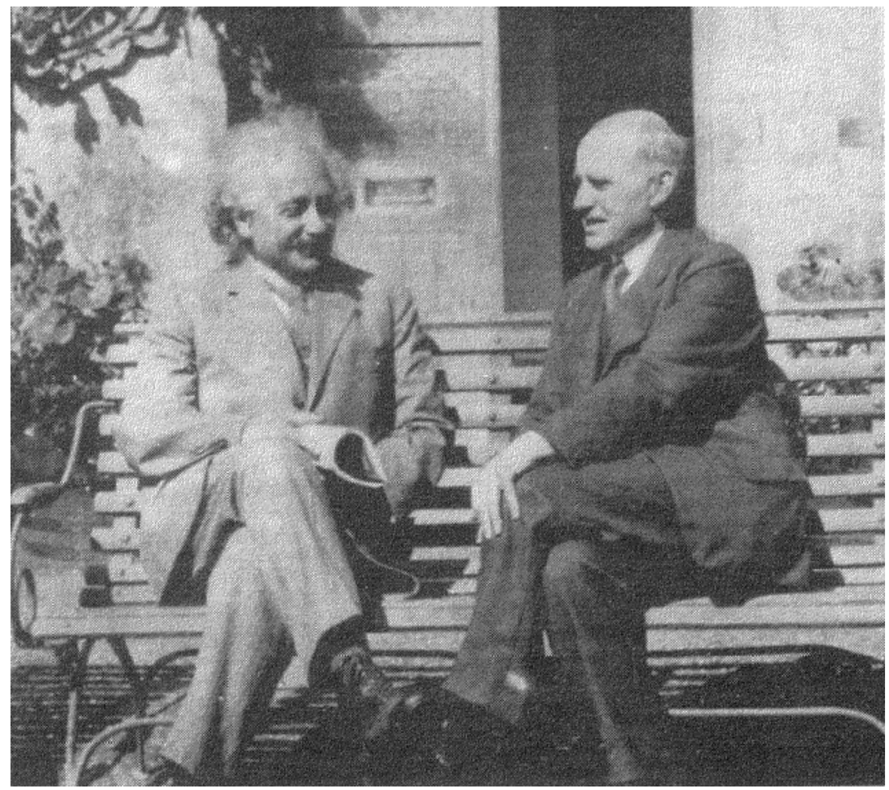

Einstein and Eddington, Cambridge, 1930

Gravitational Deflection of Light is a Well-Known Effect Today

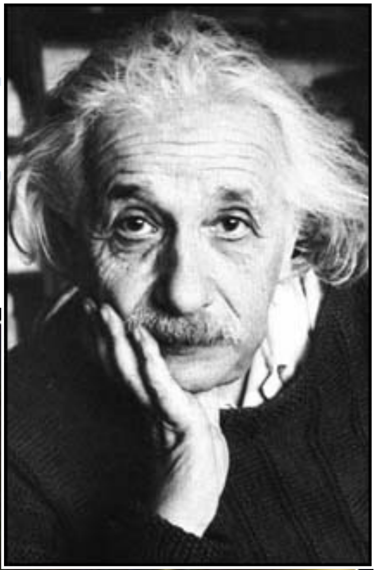

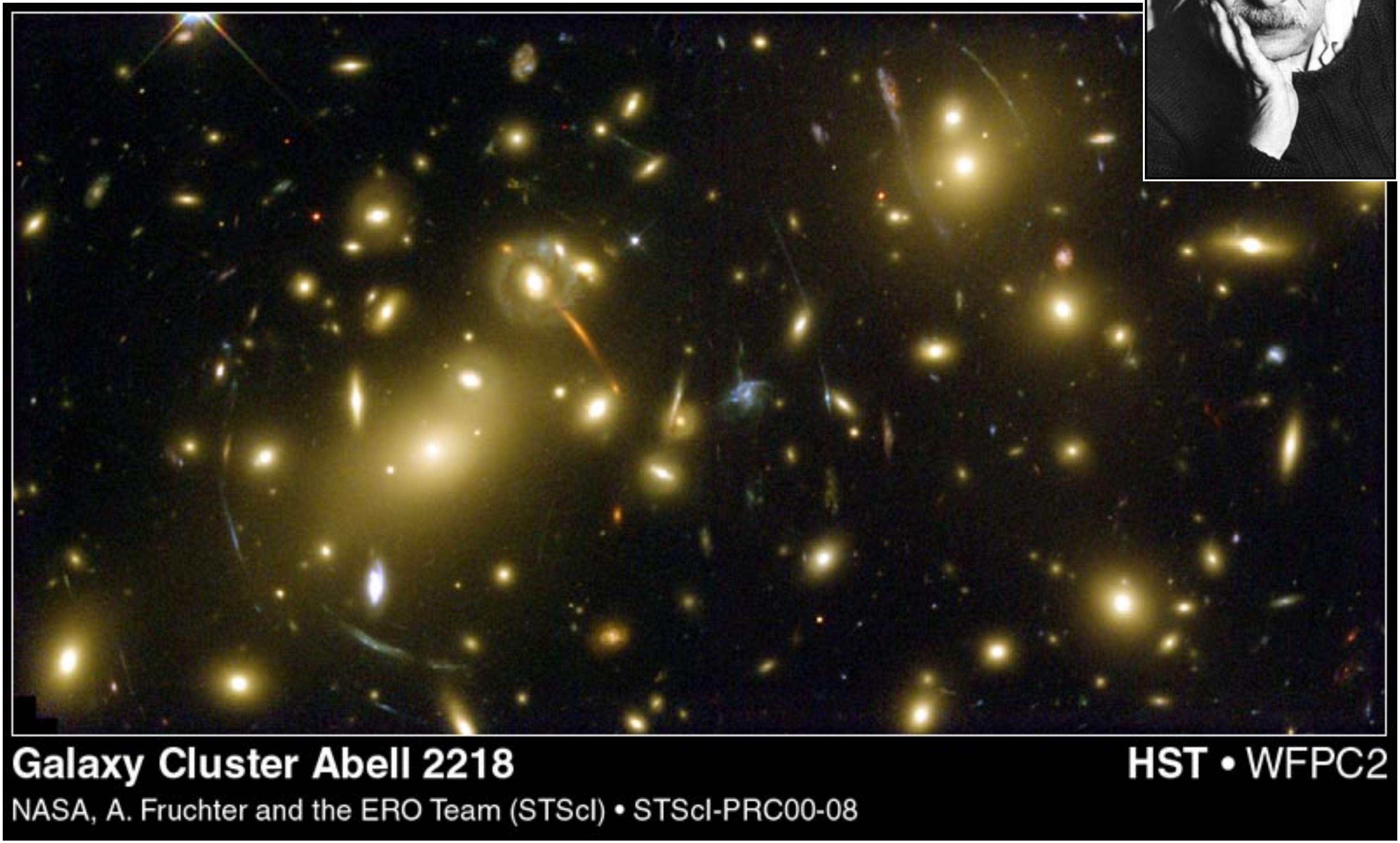

Our solar system and tests of gravity

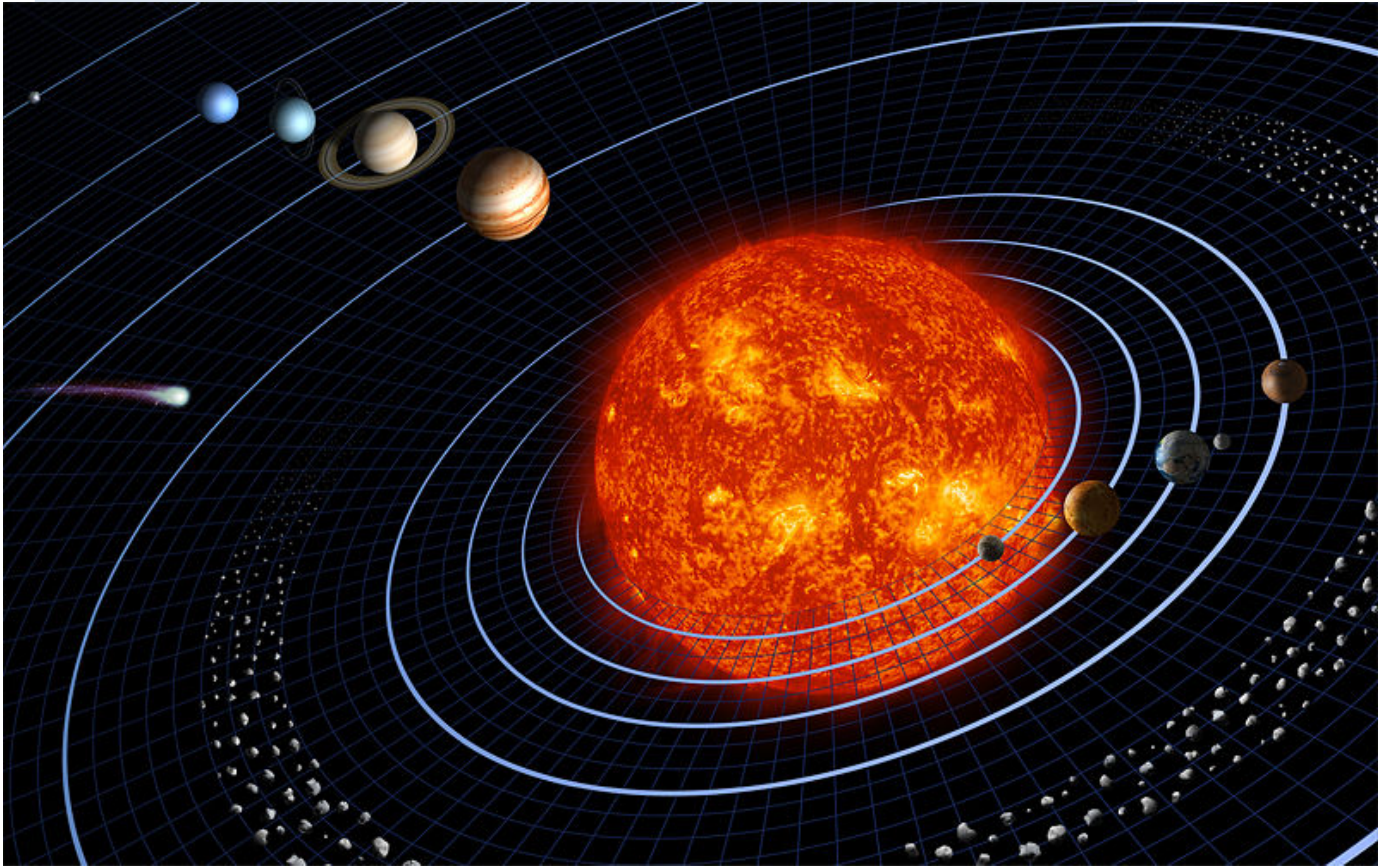

50+ Years of Solar System Gravity Tests

Techniques for Gravity Tests:

Radar Ranging:
- Planets: Mercury, Venus, Mars
- s/c: Mariners, Vikings, Pioneers, Cassini, Mars Global Surveyor, Mars Orbiter, etc.
- VLBI, GPS, etc.

Laser:
- SLR, LLR, interplanetary, etc.

Dedicated Gravity Missions:

- **LLR (1969 - on-going!!)**
- GP-A,'76; LAGEOS,'76,'92; GP-B,'04; LARES,'12; MicroSCOPE,'16, ACES, '20; LIGO,'16; eLISA, 2030+(?)

"for decisive contributions to the LIGO detector and the observation of gravitational waves"

New Engineering Discipline – Applied General Relativity:

- Daily life: GPS, geodesy, time transfer;
- Precision measurements, deep-space navigation & μas-astrometry (Gaia)

General relativity is now well tested. Can we use it to build something?

Discovery of an exoplanet around a solar-type star

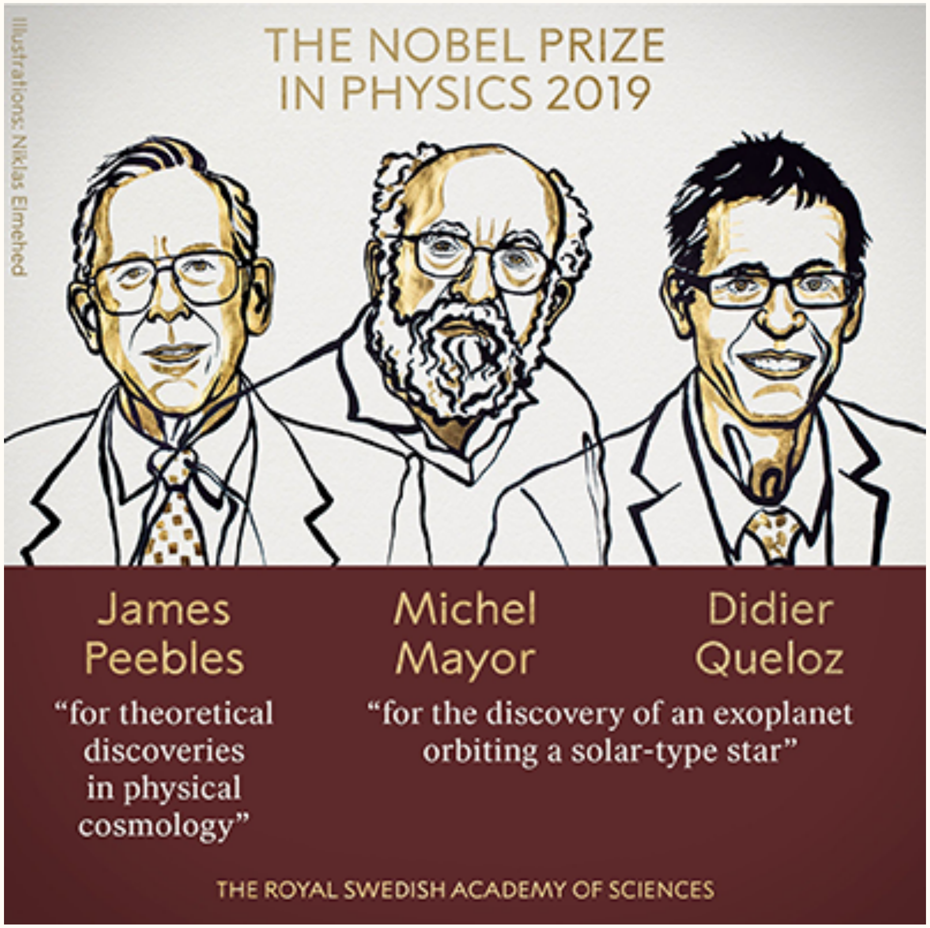

A Jupiter-mass companion to a solar-type star

Michel Mayor & Didier Queloz

Geneva Observatory, 51 Chemin des Maillettes, CH-1290 Sauverny, Switzerland

The presence of a Jupiter-mass companion to the star 51 Pegasi is inferred from observations of periodic variations in the star's radial velocity. The companion lies only about eight million kilometres from the star, which would be well inside the orbit of Mercury in our Solar System. This object might be a gas-giant planet that has migrated to this location through orbital evolution, or from the radiative stripping of a brown dwarf.

For more than ten years, several groups have been examining the radial velocities of dozens of stars, in an attempt to identify orbital motions induced by the presence of heavy planetary companions[1-5]. The precision of spectrographs optimized for Doppler studies and currently in use is limited to about $15\,\mathrm{m\,s^{-1}}$. As the reflex motion of the Sun due to Jupiter is $13\,\mathrm{m\,s^{-1}}$, all current searches are limited to the detection of objects with at least the mass of Jupiter (M_J). So far, all precise Doppler surveys have failed to detect any jovian planets or brown dwarfs.

Since April 1994 we have monitored the radial velocity of 142 G and K dwarf stars with a precision of $13\,\mathrm{m\,s^{-1}}$. The stars in our survey are selected for their apparent constant radial velocity (at lower precision) from a larger sample of stars monitored for 15 years[6,7]. After 18 months of measurements, a small number of stars show significant velocity variations. Although most candidates require additional measurements, we report here the discovery of a companion with a minimum mass of $0.5\,M_J$, orbiting at 0.05 AU around the solar-type star 51 Peg. Constraints originating from the observed rotational velocity of 51 Peg and from its low chromospheric emission give an upper limit of $2\,M_J$ for the mass of the companion. Alternative explanations to the observed radial velocity variation (pulsation or spot rotation) are unlikely.

The very small distance between the companion and 51 Peg is certainly not predicted by current models of giant planet formation[8]. As the temperature of the companion is above 1,300 K, this object seems to be dangerously close to the Jeans thermal evaporation limit. Moreover, non-thermal evaporation effects are known to be dominant[9] over thermal ones. This jovian-mass companion may therefore be the result of the stripping of a very-low-mass brown dwarf.

The short-period orbital motion of 51 Peg also displays a long-period perturbation, which may be the signature of a second low-mass companion orbiting at larger distance.

Discovery of Jupiter-mass companion(s)

Our measurements are made with the new fibre-fed echelle spectrograph ELODIE of the Haute-Provence Observatory, France[10]. This instrument permits measurements of radial velocity with an accuracy of about $13\,\mathrm{m\,s^{-1}}$ of stars up to 9 mag in an exposure time of <30 min. The radial velocity is computed

Imaging Exoplanets with the Solar Gravitational Lens

Credit: J. DeLuca

THE SOLAR GRAVITATIONAL LENS

Imaging point sources with the SGL

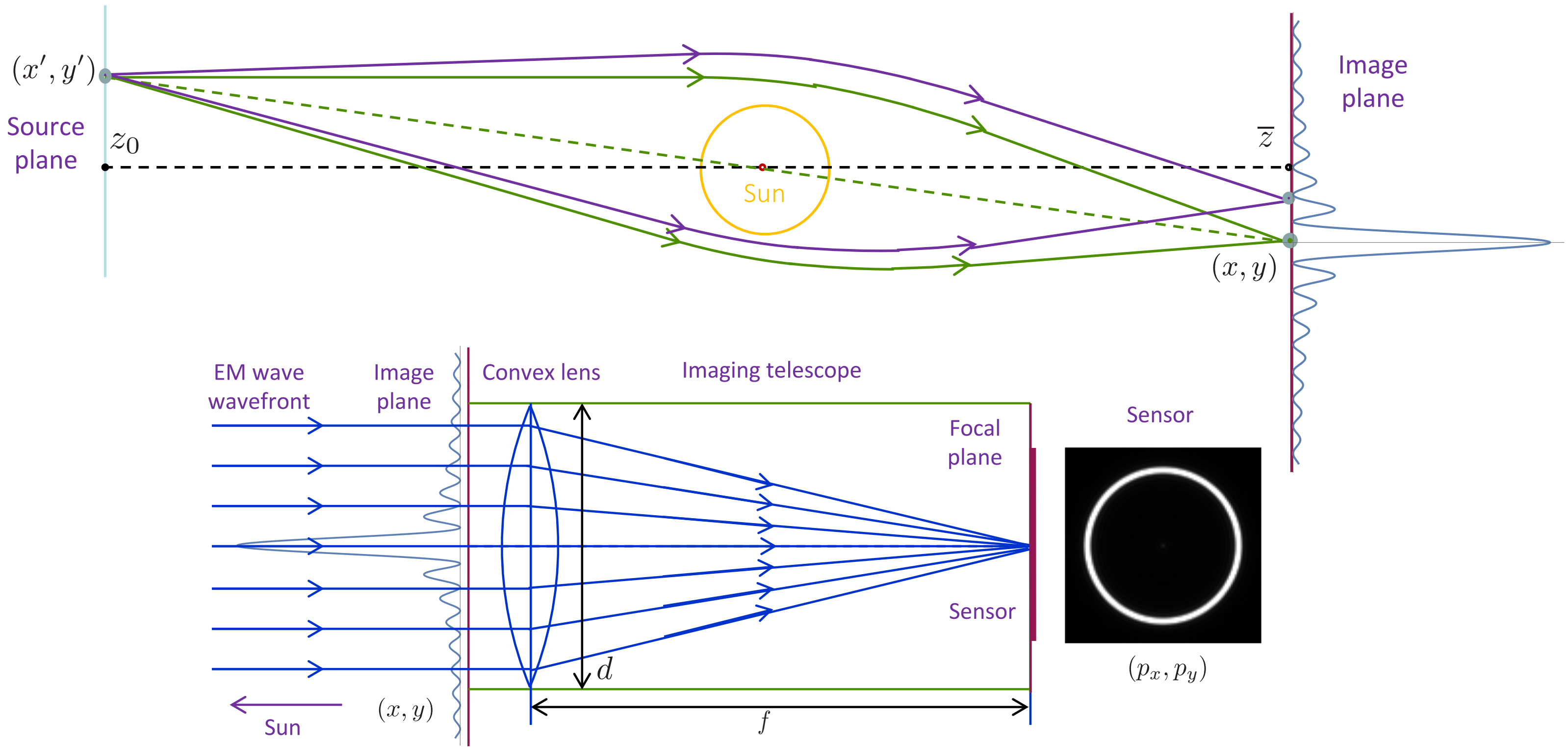

$\rho_0 = 0$

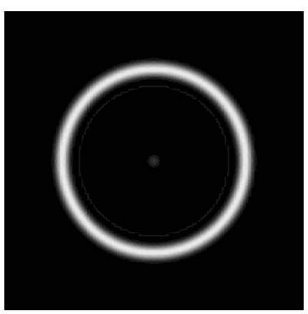

On-axis

$0 < \rho_0 \ll 2 \text{ cm}$

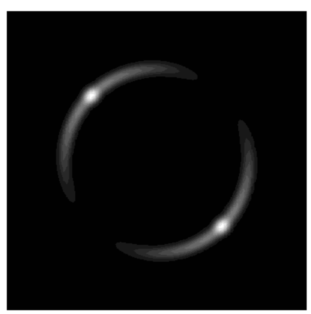

Small off-axis displacement

$0.5\,\text{m} \lesssim \rho_0 \lesssim r_g$

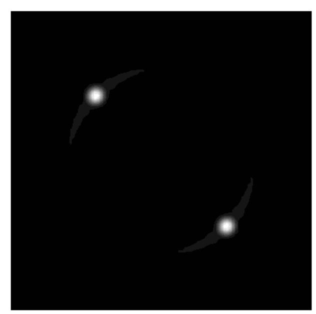

Large off-axis displacement

$\rho_0 \gtrsim R_\odot$

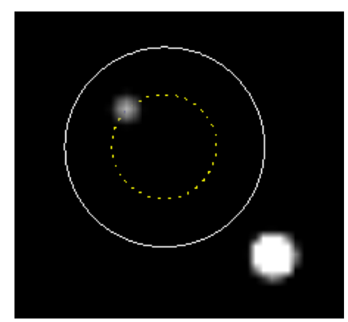

Very large off-axis displacement

Image formation process with the SGL

Image formation for an extended source

$B_s(\mathbf{x}')$

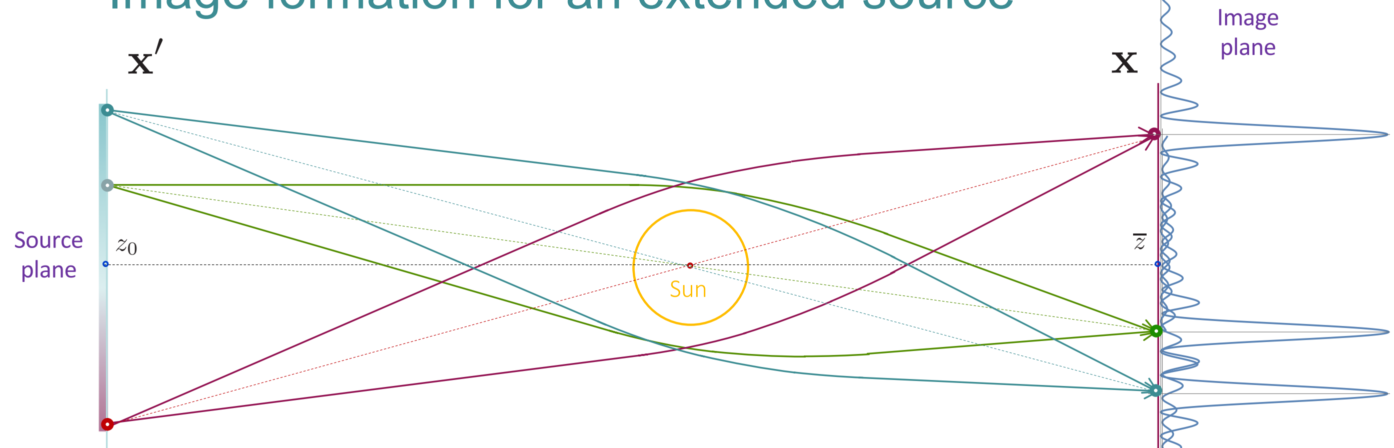

$I_0(\mathbf{x})$

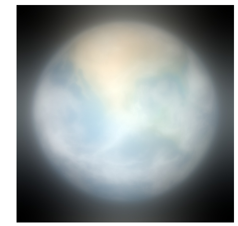

$$I_0(\mathbf{x}) \;=\; \frac{2\pi}{z_0^2}\frac{r_g}{\lambda}\iint\limits_{-\infty}^{+\infty} d^2\mathbf{x}'\, B_s(\mathbf{x}')\, J_0^2\Big(\frac{2\pi}{\lambda}\sqrt{\frac{2r_g}{z}}\big|\mathbf{x}+\frac{z}{z_0}\mathbf{x}'\big|\Big)$$

3-D description of imaging

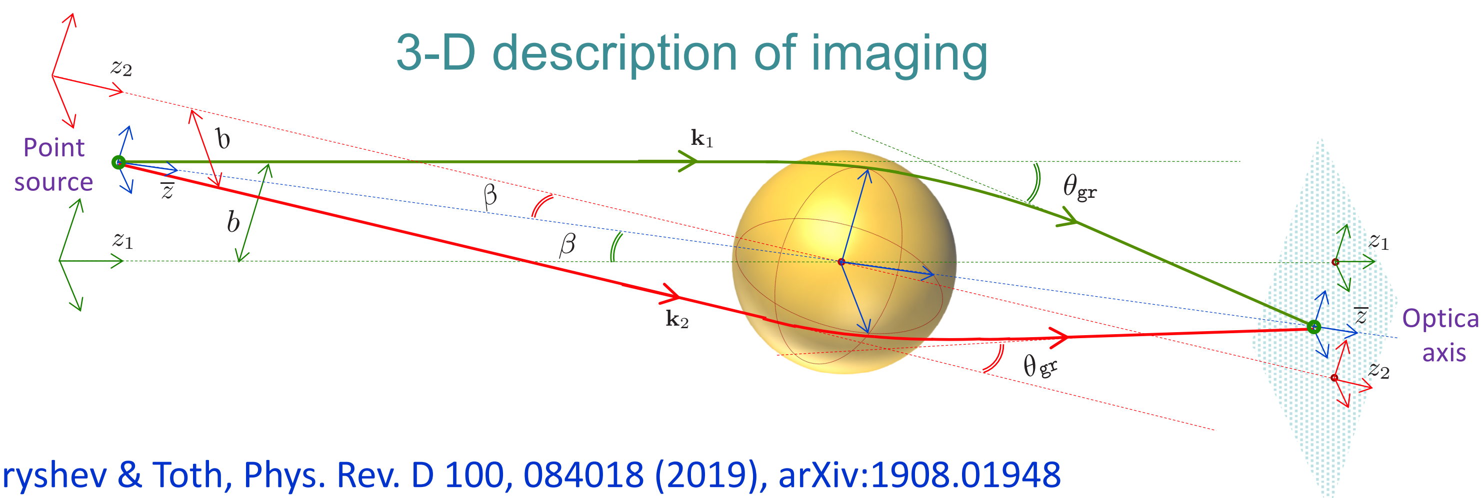

Turyshev & Toth, Phys. Rev. D 100, 084018 (2019), arXiv:1908.01948

Modeling the signal from an extended source

Power from directly imaged region: $P_{\tt dir}(r_0) = B_s\pi(\tfrac{1}{2}d)^2 \frac{d}{4\overline{z}}\sqrt{\frac{2r_g}{\overline{z}}}$.

Power from the rest of the planet (blur):

$$P_{\tt blur}(r_0) = P_{\tt dir}(r_0)\Big(\frac{2R_\oplus}{d}\frac{\overline{z}}{z_0}\epsilon(r_0) - 1\Big)$$

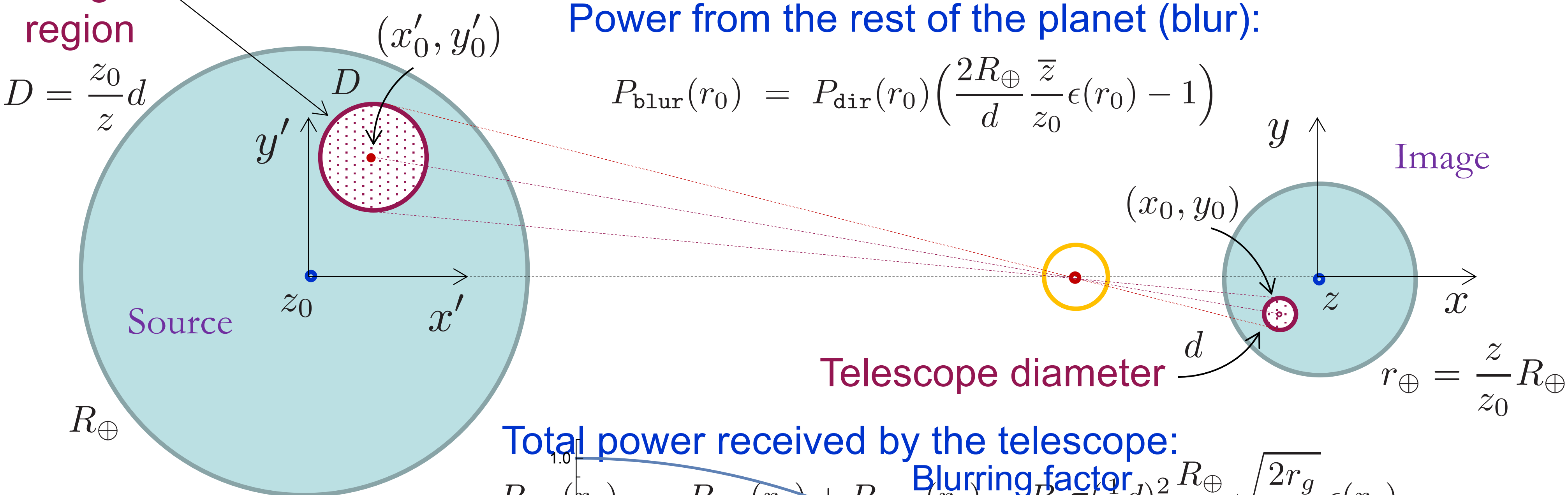

Total power received by the telescope:

$$P_{\tt exo}(r_0) = P_{\tt dir}(r_0) + P_{\tt blur}(r_0) = B_s\pi(\tfrac{1}{2}d)^2 \frac{R_\oplus}{2z_0}\sqrt{\frac{2r_g}{\overline{z}}}\,\epsilon(r_0)$$

Blurring factor

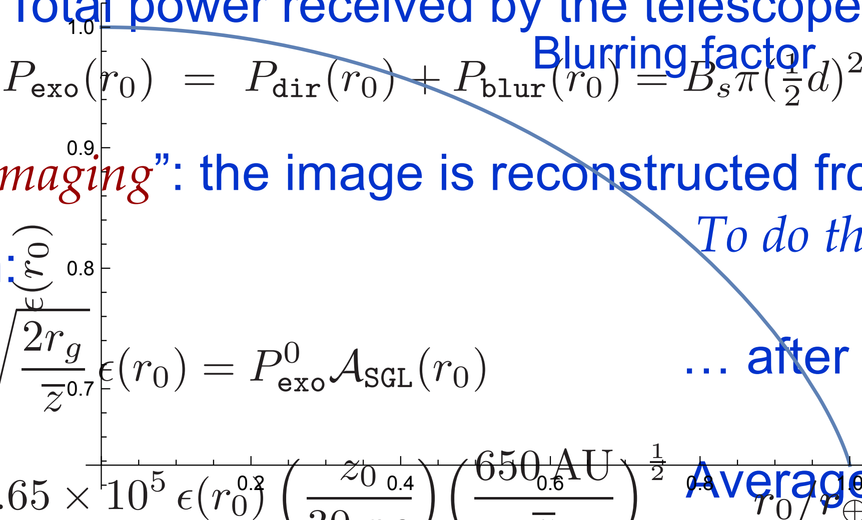

"*Shadow imaging*": the image is reconstructed from variations of blur.

To do that we need high SNR!

Interesting observation:

$$P_{\tt exo}(r_0) = B_s\pi(\tfrac{1}{2}d)^2 \frac{R_\oplus}{2z_0}\sqrt{\frac{2r_g}{\overline{z}}}\,\epsilon(r_0) = P^0_{\tt exo}\mathcal{A}_{\tt SGL}(r_0)$$

… after re-arranging terms

$$\mathcal{A}_{\tt SGL}(r_0) = \frac{z_0}{2R_\oplus}\sqrt{\frac{2r_g}{\overline{z}}}\,\epsilon(r_0) = 5.65\times 10^5\,\epsilon(r_0)\Big(\frac{z_0}{30\ \mathrm{pc}}\Big)\Big(\frac{650\,\mathrm{AU}}{\overline{z}}\Big)^{\frac{1}{2}}$$

Averaged SGL amplification is wavelength independent!

Photon flux received from exo-Earth

Photon rate: $$Q_{\tt exo} = \frac{\lambda\epsilon_\lambda}{hc}\, a I_\odot \frac{\pi d^2}{4}\frac{R_\oplus}{z_0}\sqrt{\frac{2r_g}{z}}$$

ϵ - correction for solar spectral irradiance

$$\epsilon_{\tt vis} = 0.5 \qquad \epsilon_{\tt IR} = 0.4 \qquad \epsilon_{\tt UV} = 0.1$$

Image diameter:

$$2r_\oplus = 1.3\Big(\frac{z}{650\ \mathrm{AU}}\Big)\Big(\frac{30\ \mathrm{pc}}{z_0}\Big)\ \mathrm{km}$$

Maximum SNR per imaged pixel:

$$\mathrm{SNR}_{\tt R}^{\tt max} = \frac{2r_\oplus}{d}\cdot \mathrm{SNR}_{\tt S}$$

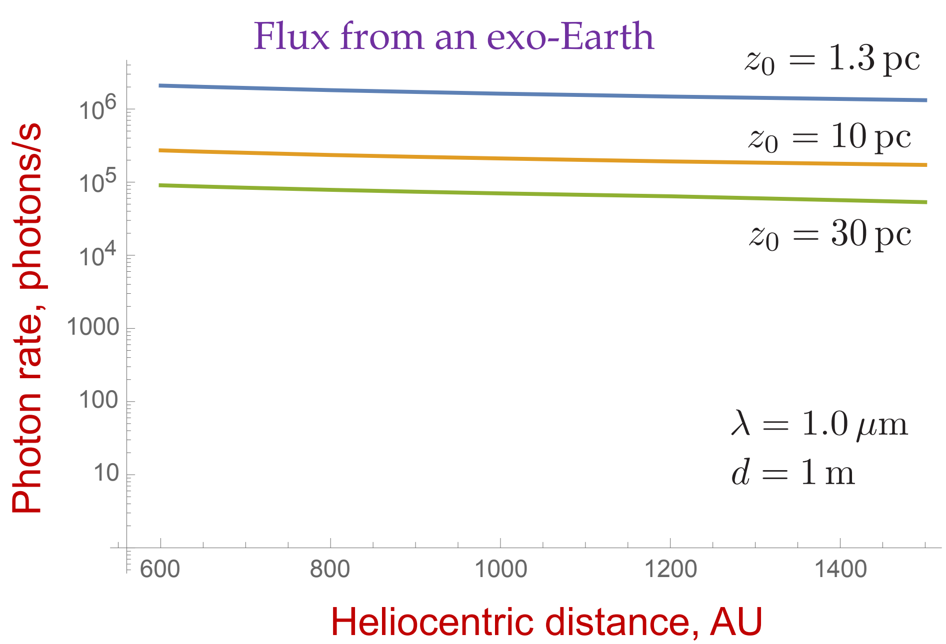

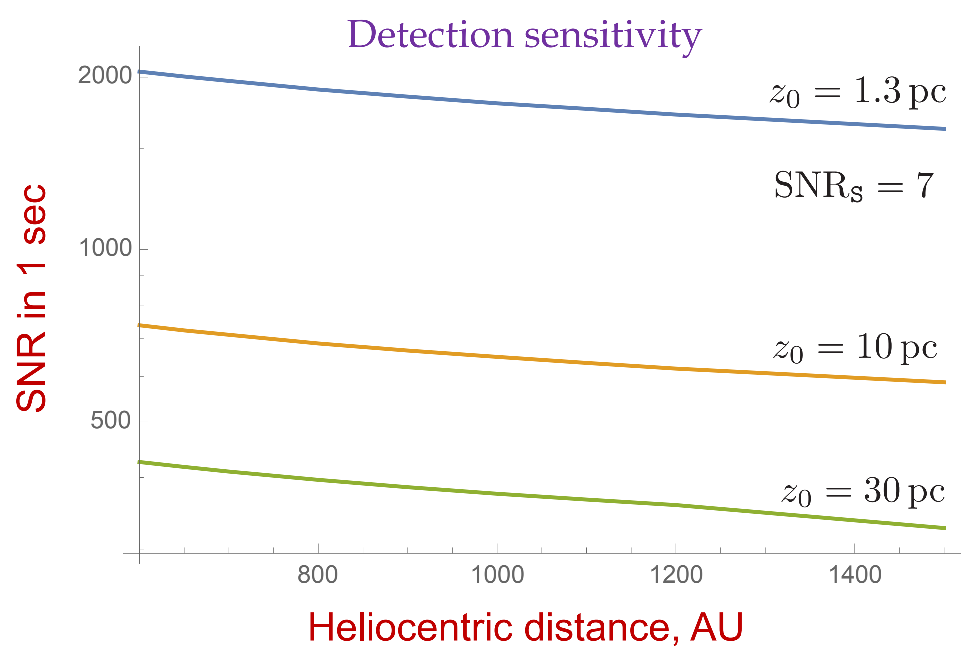

Amplified signal from distant exoplanets may be used for imaging

Convolving BW source with the SGL

An image of the Earth with
1024 x 1024 pixels

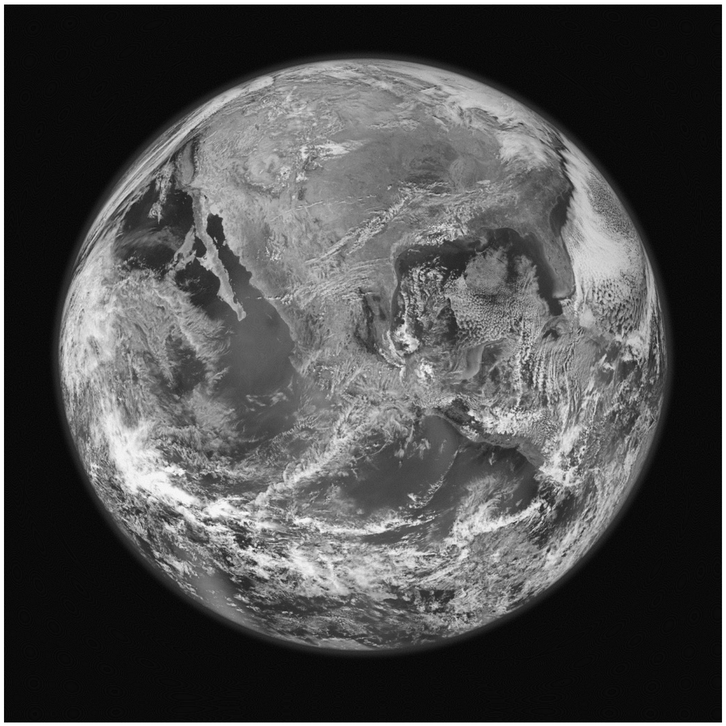

Some source features
are still recognizable

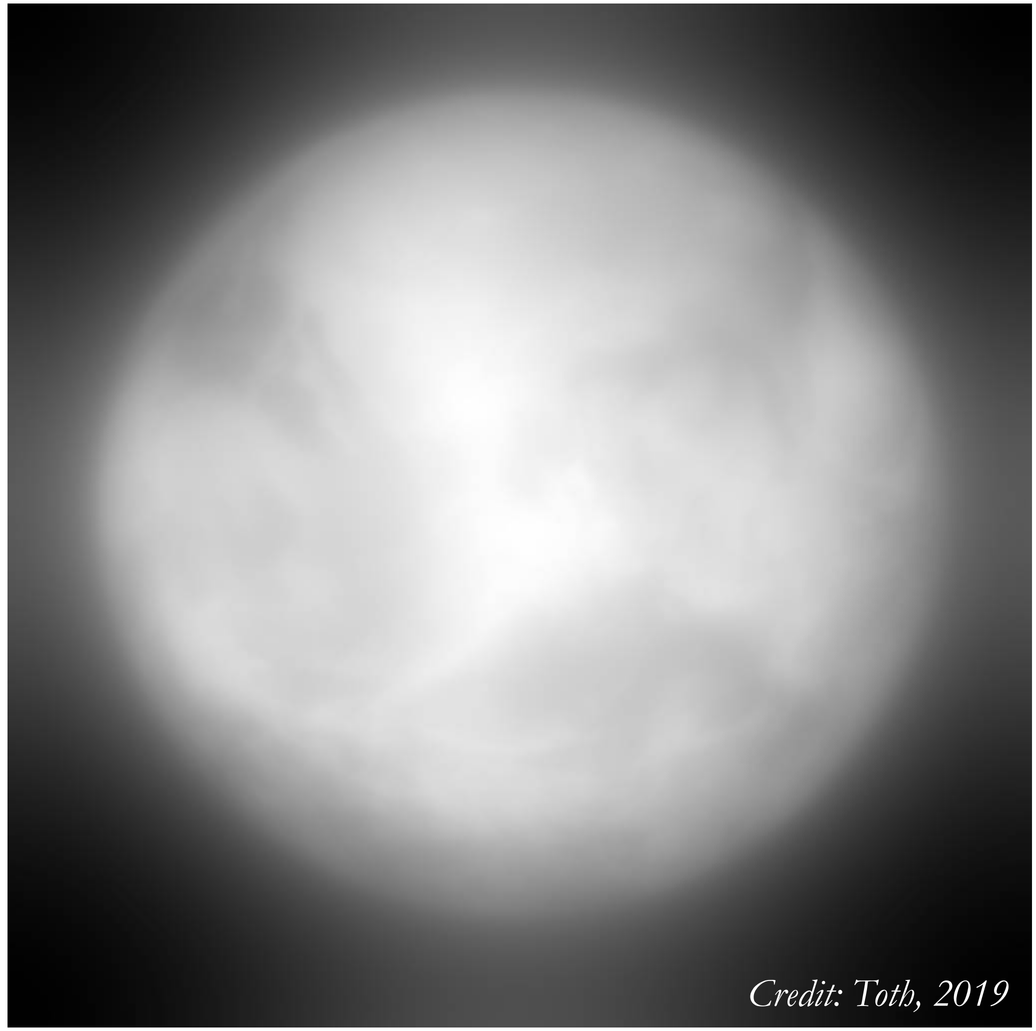

The convolved image of an exo-Earth at 30pc,
formed by the SGL at z = 650 AU, with λ = 500 nm

SGL Image Deconvolution

Credit: Toth, 2019

An image of the Earth with
1024 x 1024 pixels

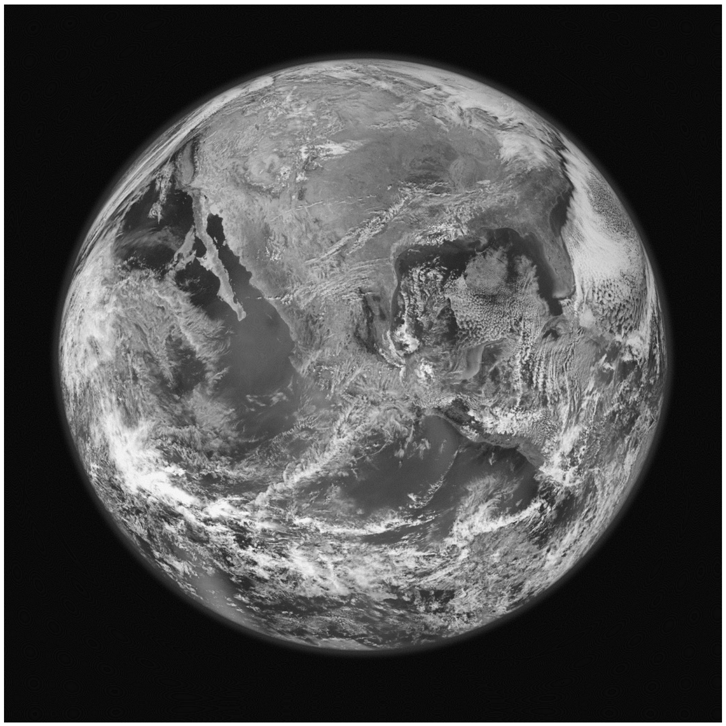

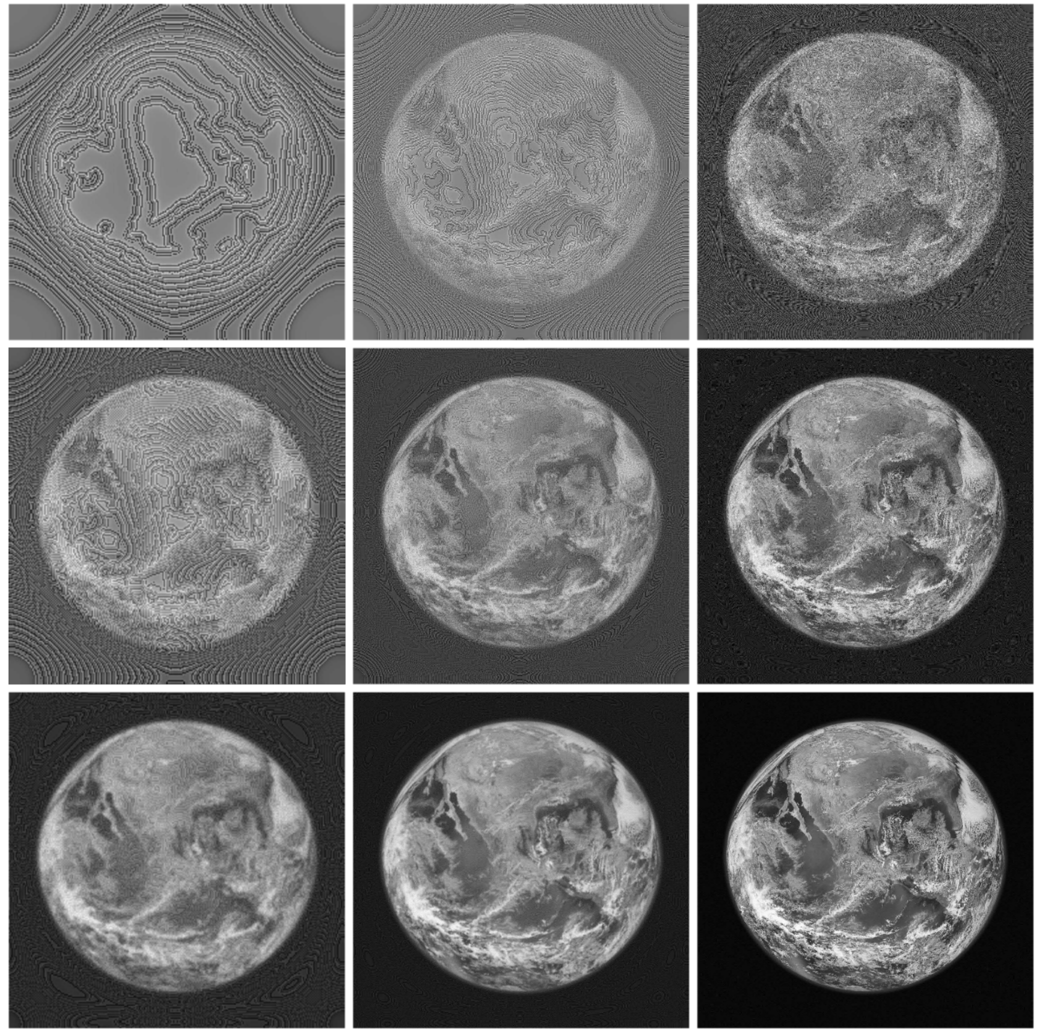

Right: Deconvolution at different resolutions and bit depths. Columns: resolutions of (256x256), (512x512), (1024x1024) pixels. Rows: “low quality” (4, 6, 8 bits), “medium quality" (6, 8, 10 bits), “high quality” (8, 10, 12 bits) samples.

Convolving source with the SGL (color)

As the telescope aperture is much larger than the first minimum of the PSF, the actual SGL's magnification is <u>wavelength independent</u>!

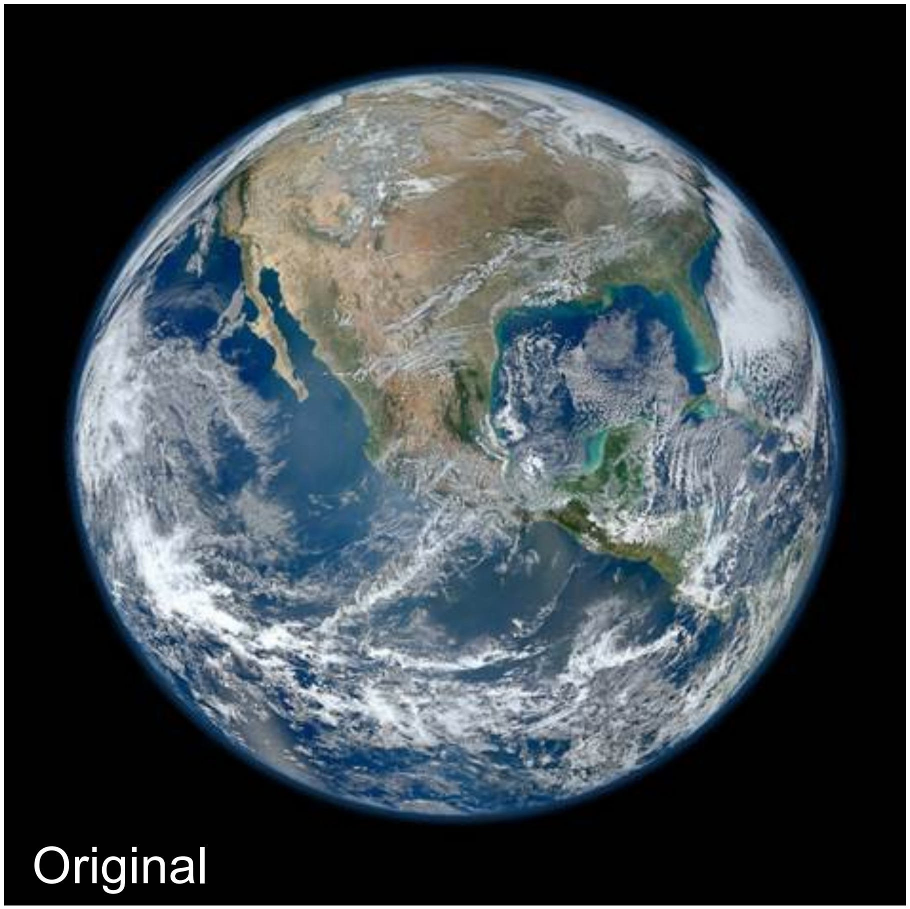

Major features are clearly visible. Spatially resolved spectroscopy is possible.

Deconvolving broadband images

As the telescope aperture is much larger than the first minimum of the PSF, the actual SGL's magnification is <u>wavelength independent</u>!

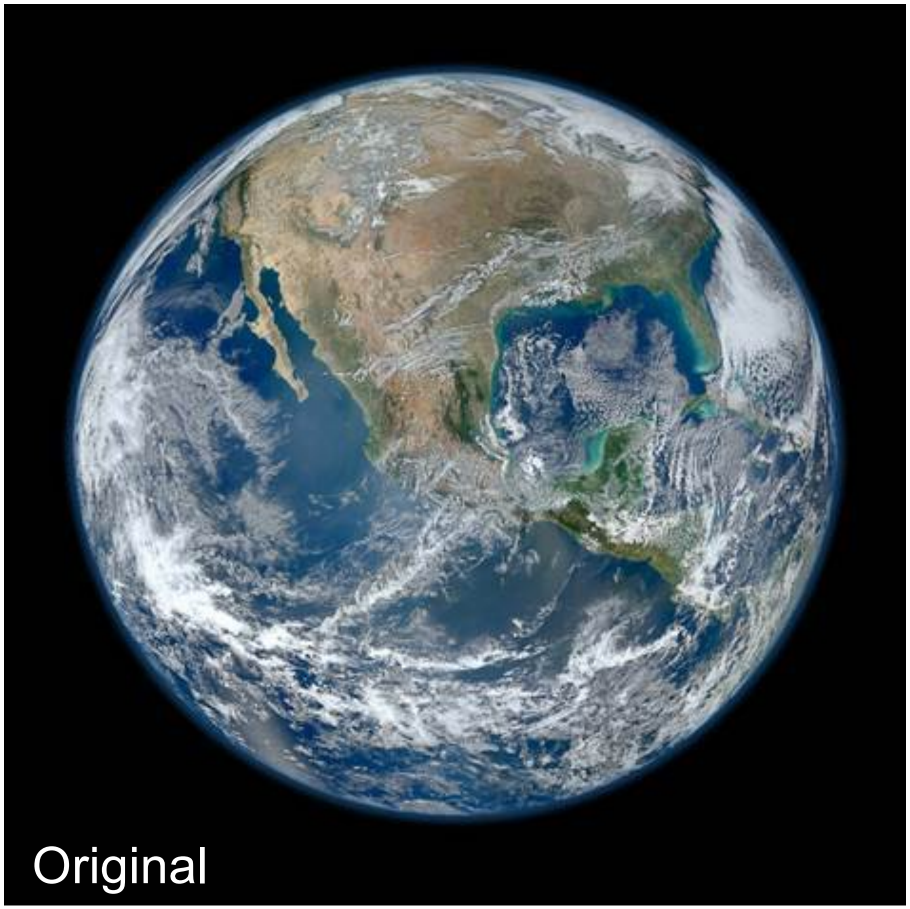

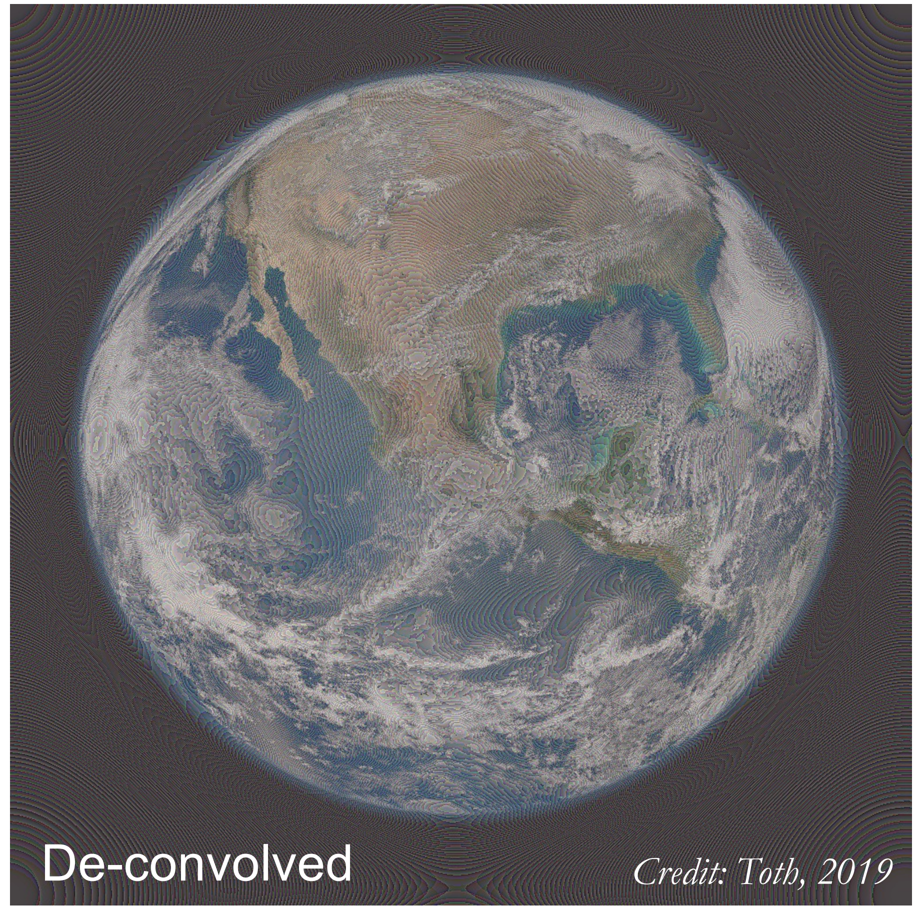

Initial convolution/deconvolution results are promising. Further work is needed.

Do not point at the Sun!!!!

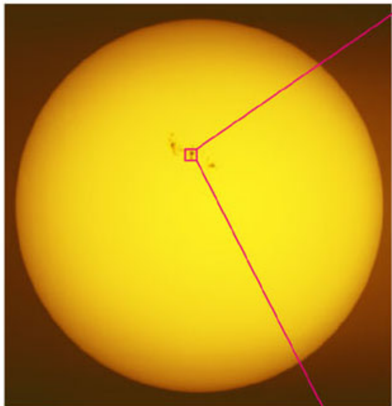

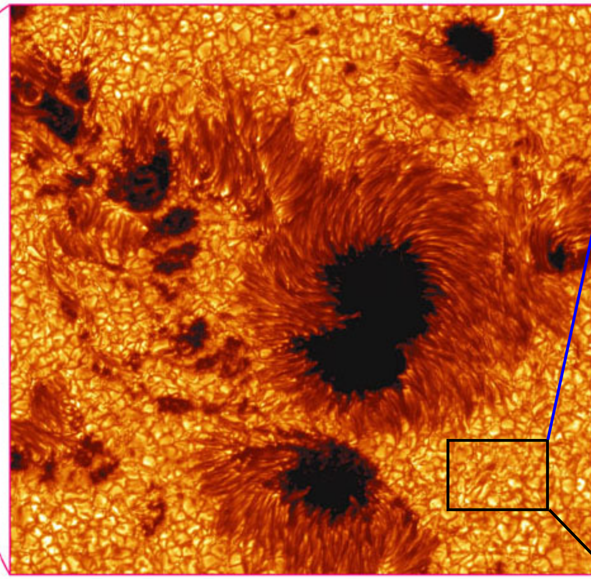

Granulation of solar surface

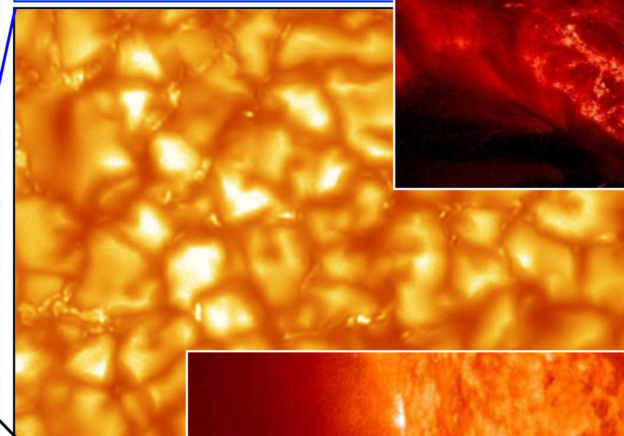

A solar flare

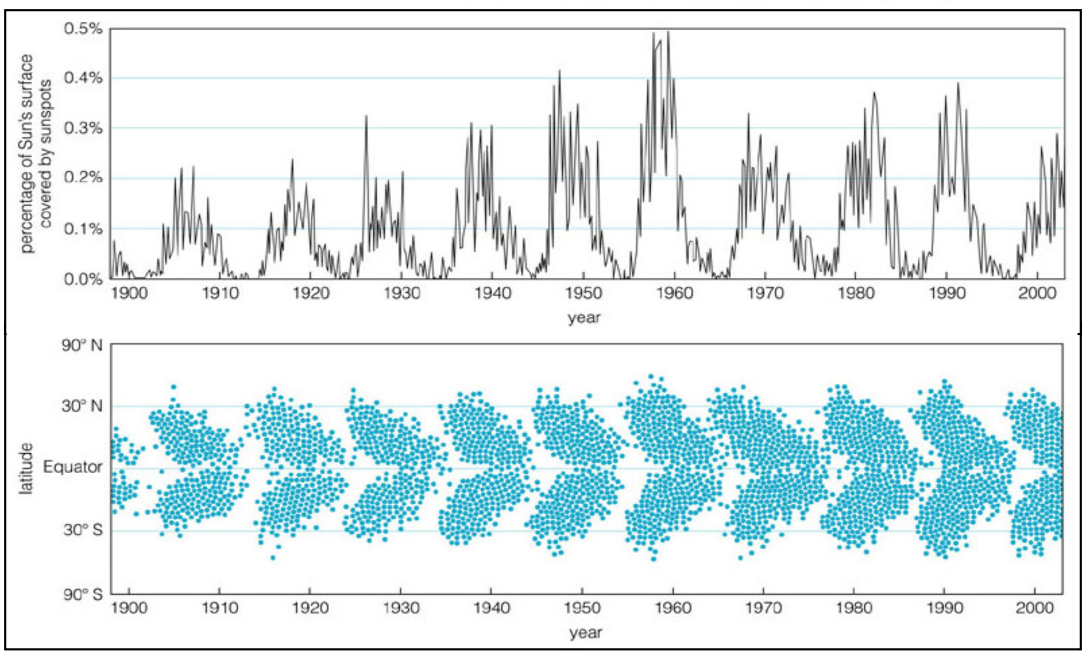

Coronal mass ejection

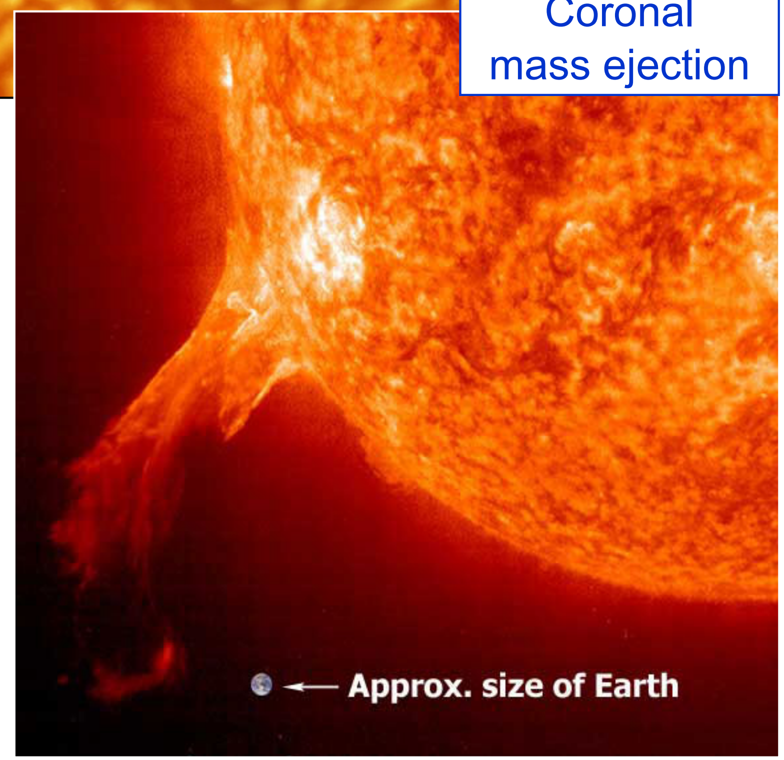

Plasma contribution to SGL

For SGL-relevant geometry, wave effects on light propagation are negligible

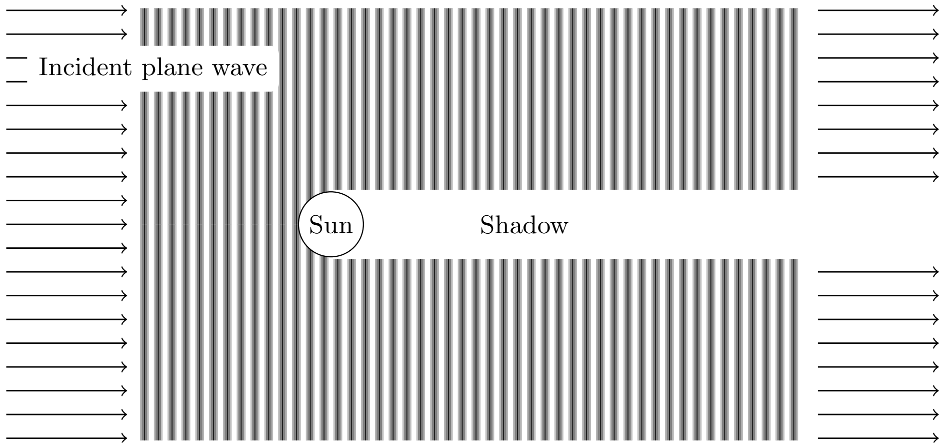

Spherical obscuration

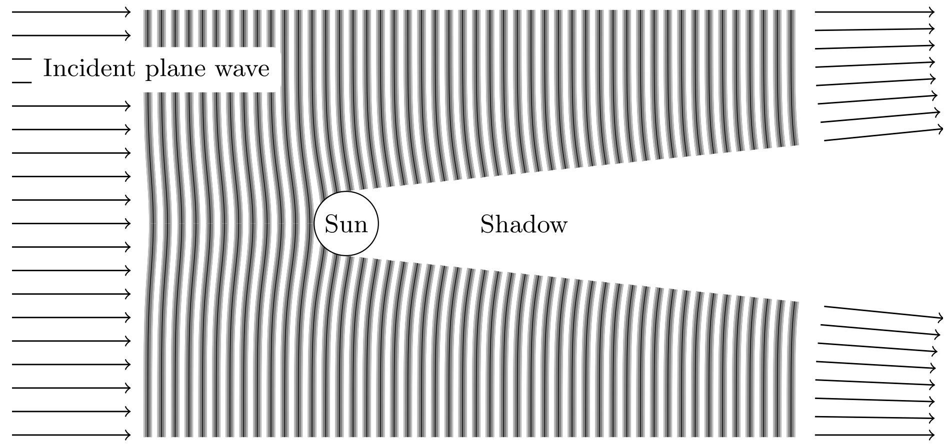

Plasma only

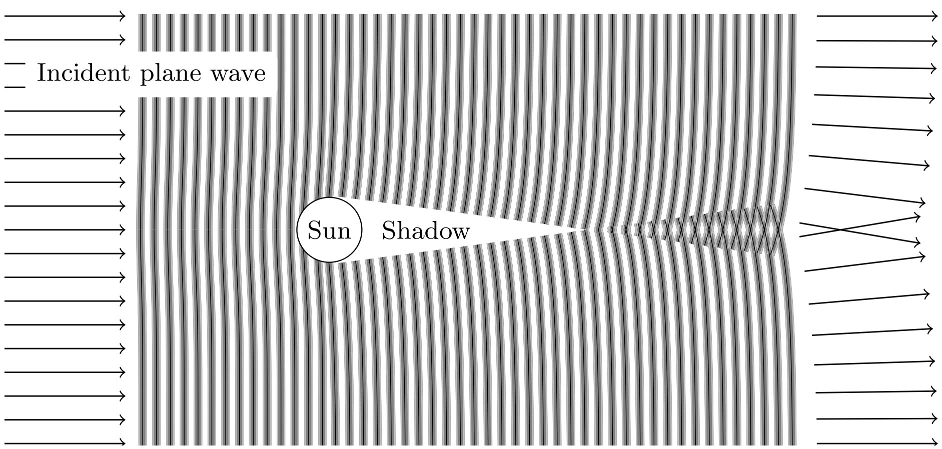

Pure gravity

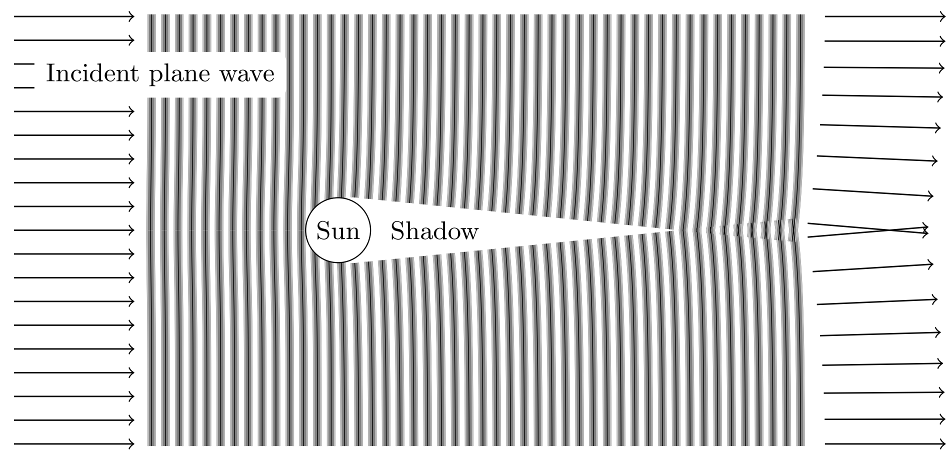

Gravity + Plasma

Plasma pushes the focal area of the SGL outward to higher heliocentric ranges

Effect of solar corona on light amplification

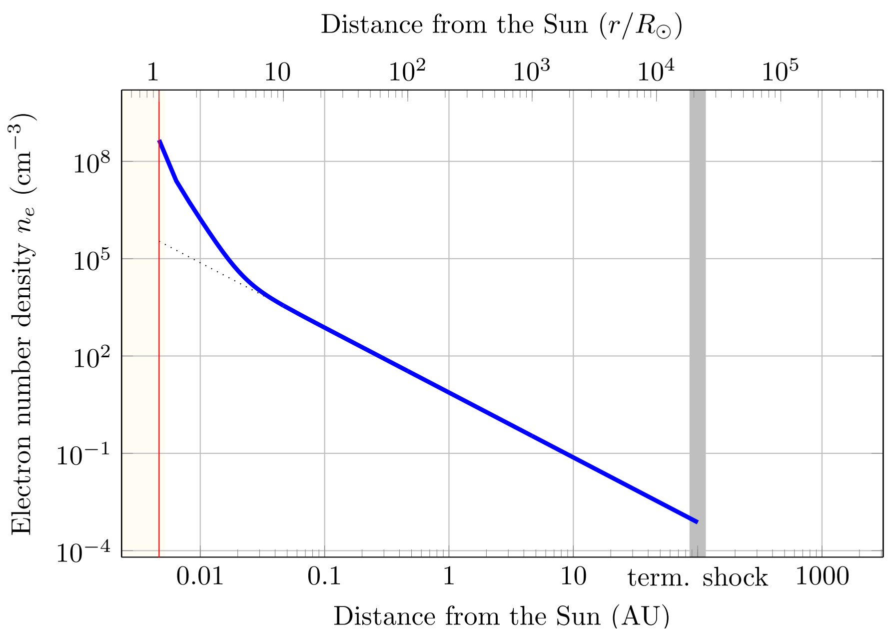

Turyshev & Toth, Phys. Rev. D 99, 024044 (2019)

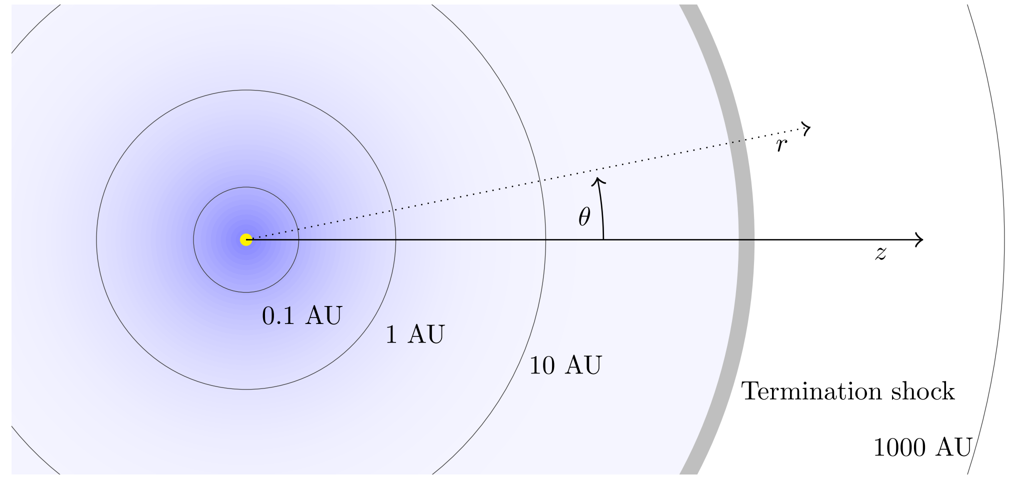

Solar corona electron content density (Muhleman et al., 1977):

$$\overline{n}_e(r) = \Big[2.99\times10^8\Big(\frac{R_\odot}{r}\Big)^{16} + 1.55\times10^8\Big(\frac{R_\odot}{r}\Big)^{6} + 3.44\times10^5\Big(\frac{R_\odot}{r}\Big)^{2}\Big]\ \mathrm{cm}^{-3}. \quad\Rightarrow\quad \omega_\mathrm{p}^2 = \frac{4\pi e^2}{m_e}\sum_i \alpha_i\Big(\frac{R_\odot}{r}\Big)^{\beta_i}$$

$$\bar{\mu}_z = \frac{4\pi^2}{1-e^{-4\pi^2 r_g/\lambda}}\frac{r_g}{\lambda}\mathcal{F}_\mathrm{pg}^2 J_0^2\Big(2\pi\frac{\rho}{\lambda}\sqrt{\frac{2r_g}{z}}\mathcal{F}_\mathrm{pg}\Big)$$

SGL's point-source magnification in the presence of plasma in the solar corona

$$\mathcal{F}_\mathrm{pg} = \Big(1+\frac{\delta\theta_\mathrm{p}^2}{\delta\theta_\mathrm{g}^2}\Big)^{\frac{1}{2}} - \frac{\delta\theta_\mathrm{p}}{\delta\theta_\mathrm{g}} \geq 0 \qquad \frac{\delta\theta_\mathrm{p}}{\delta\theta_\mathrm{g}} = \Big\{7.80\times10^{-8}\Big(\frac{R_\odot}{b}\Big)^{15} + 2.41\times10^{-8}\Big(\frac{R_\odot}{b}\Big)^{5} + 2.85\times10^{-11}\Big(\frac{R_\odot}{b}\Big)\Big\}\Big(\frac{\lambda}{1\ \mu\mathrm{m}}\Big)^2$$

For impact parameters $b\in[R_\odot, 3R_\odot]$, wavelengths $\lambda \geq 3\,\mathrm{cm}$ are severely affected, wavelengths $\lambda\geq 30\,\mathrm{cm}$ are completely blocked by the plasma, obliterating SGL.

Propagation of visible/IR wavelengths practically is not affected by the solar plasma

Solar corona brightness

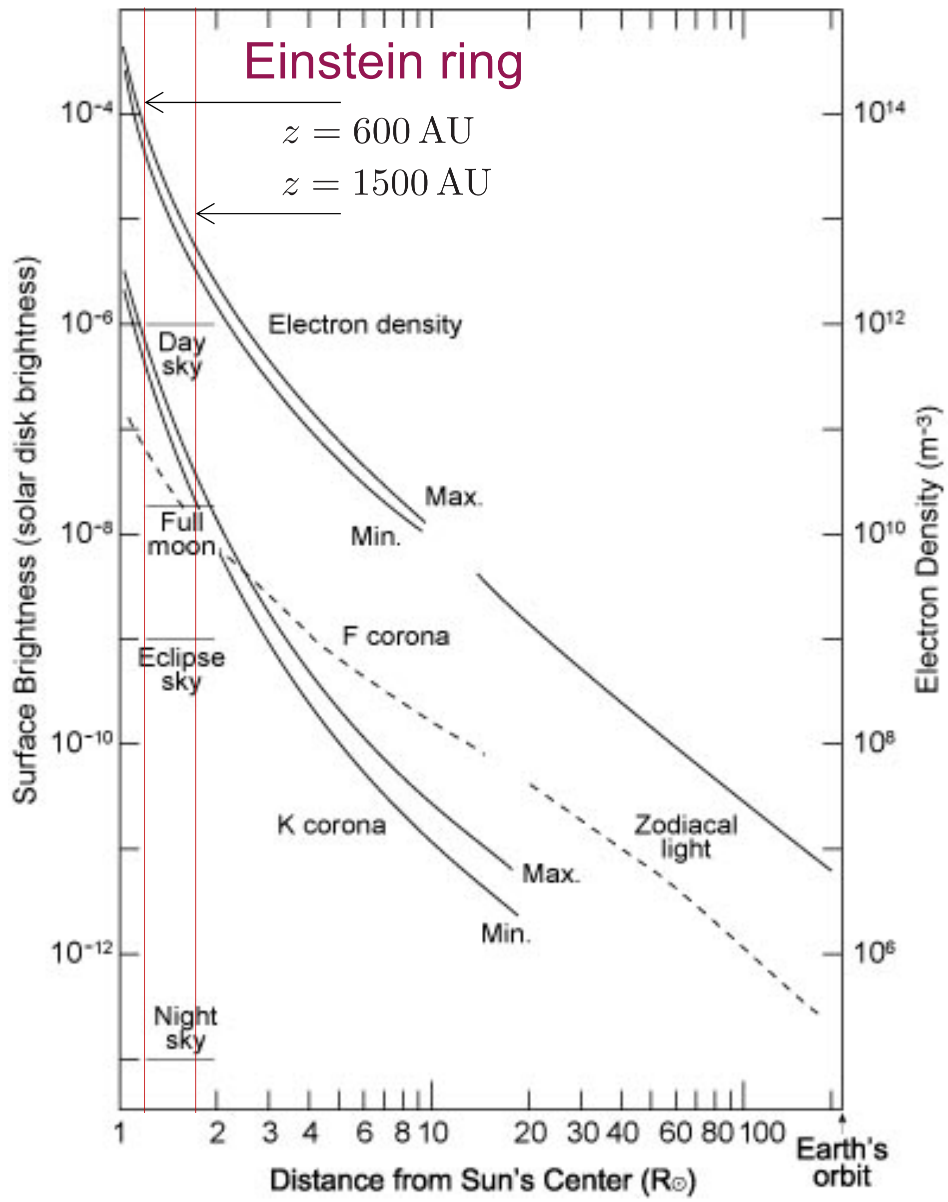

K-corona dominates for $b < 2R_\odot$

Large format imaging detector

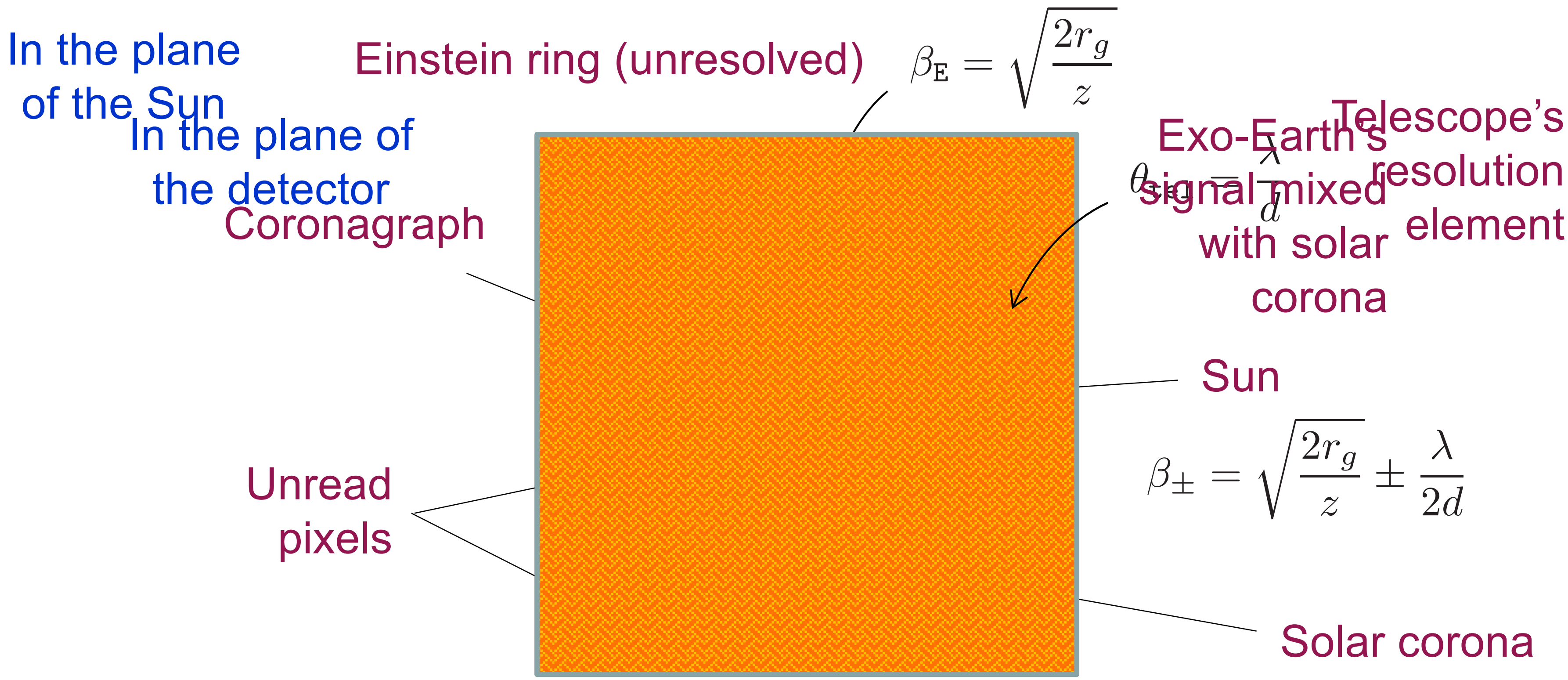

- Assumptions:
  - Coronagraph blocks-out the Sun to the level of the solar corona
  - Detector receives light from an exoplanet and that from the solar corona
  - We image the disk centered at the Einstein ring having thickness of λ/d
  - Extra pixels on the detector are not used for imaging

Brightness of the solar corona

Model for the solar corona brightness from November & Koutchumi (1996)

$$B_{\tt cor}(r) \;=\; 20.09\left(\frac{3.670}{r^{18}}+\frac{1.939}{r^{7.8}}+\frac{0.0551}{r^{2.5}}\right)\frac{\rm W}{\rm m^2\,sr} \qquad r=\frac{\overline{r}}{R_\odot}$$

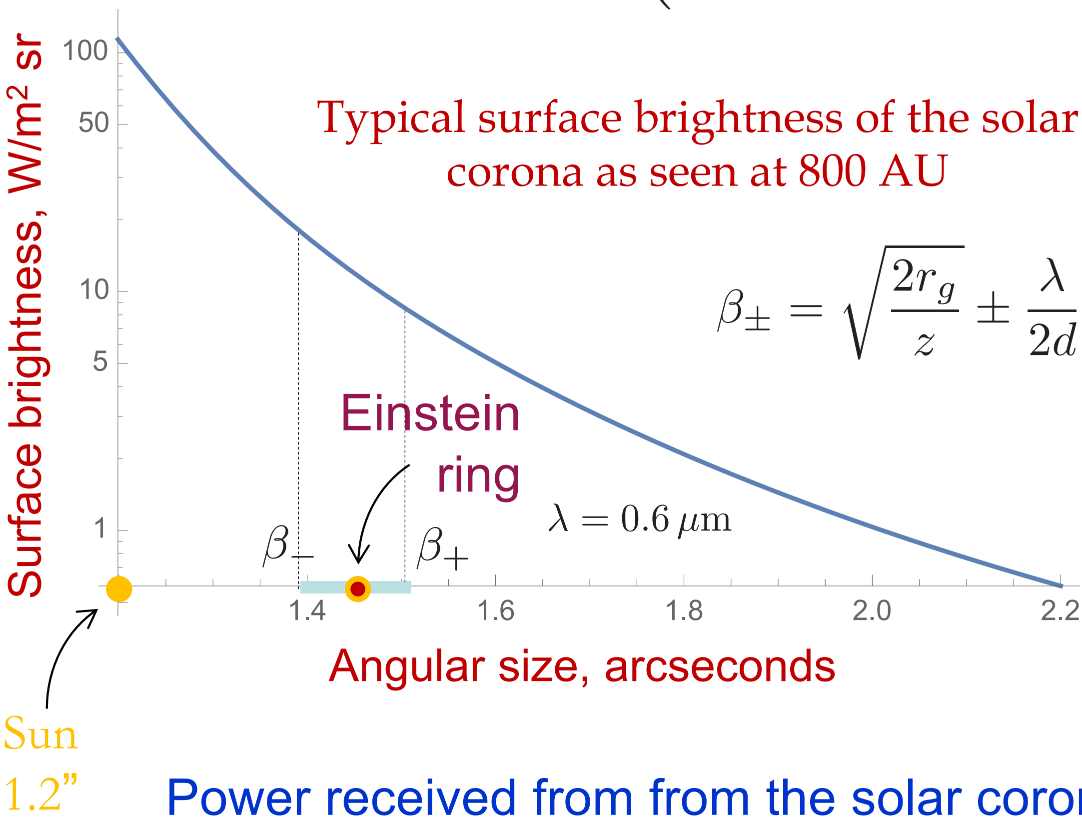

$$\beta_\pm = \sqrt{\frac{2r_g}{z}} \pm \frac{\lambda}{2d}$$

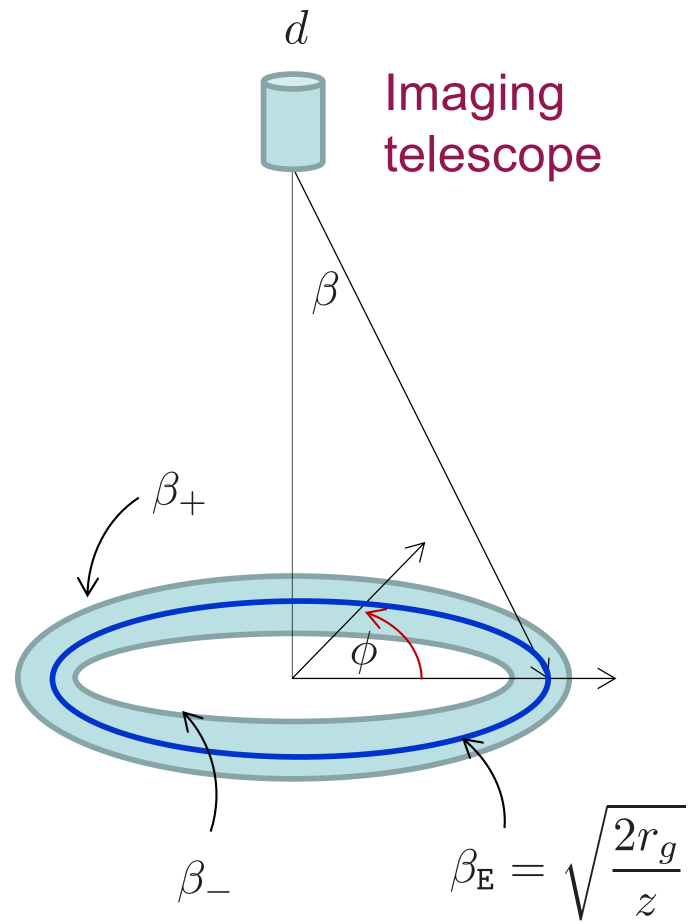

Power received from from the solar corona

$$P_{\tt cor} \;=\; \tfrac{1}{4}\pi d^2 \int_0^{2\pi} d\phi \int_{\beta_-}^{\beta_+} \beta d\beta\, B_{\tt cor}(\beta)$$

Relevant angular sizes

Thickness of the imaged region around the Sun

Relevant angular sizes as a function of heliocentric distance

$$\beta_\pm = \sqrt{\frac{2r_g}{z}} \pm \frac{\lambda}{2d}$$

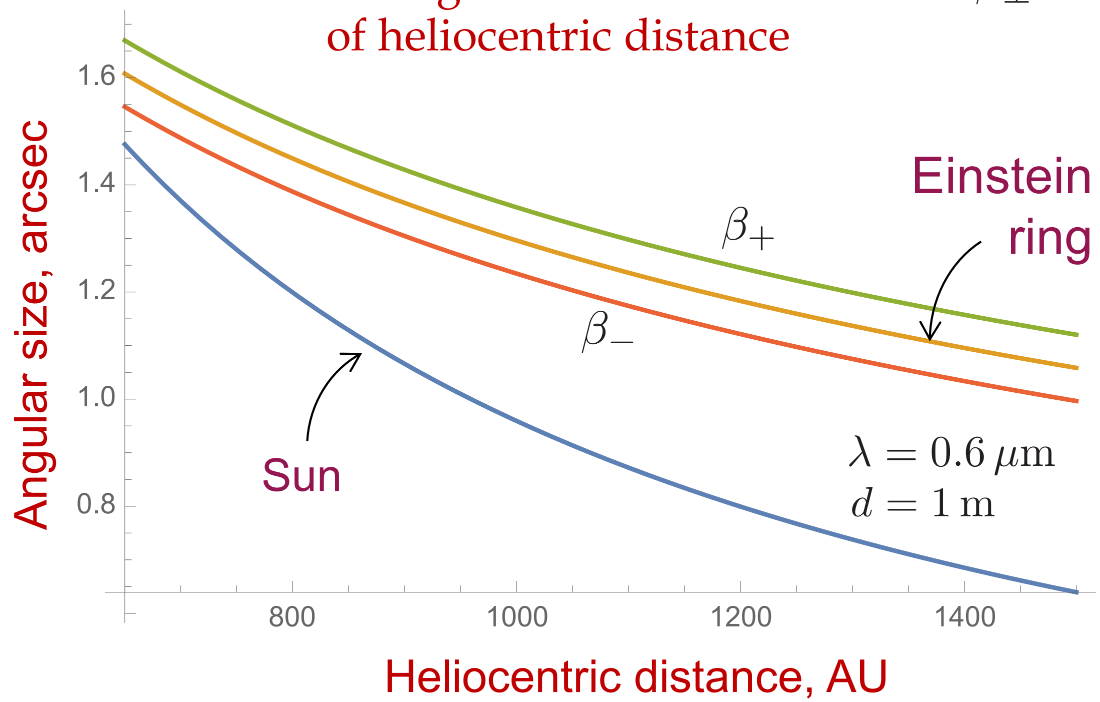

- As the heliocentric distance increases, the Einstein ring (together with the entire imaged region) further separates from the Sun. Fewer detector pixels used.
- Coronagraph may have to be able to compensate for decreasing angular sizes.

Received photon fluxes

Fluxes from the solar corona and an exoplanet

$$Q_{\mathtt{cor}} = \frac{\lambda\epsilon_\lambda}{hc}\,\tfrac{1}{4}\pi d^2 \int_0^{2\pi} d\phi \int_{\beta_-}^{\beta_+} \beta d\beta\, B_{\mathtt{cor}}(\beta) \qquad Q_{\mathtt{exo}} = \frac{\lambda\epsilon_\lambda}{hc}\, aI_\odot \frac{\pi d^2}{4}\frac{R_\oplus}{z_0}\sqrt{\frac{2r_g}{z}}$$

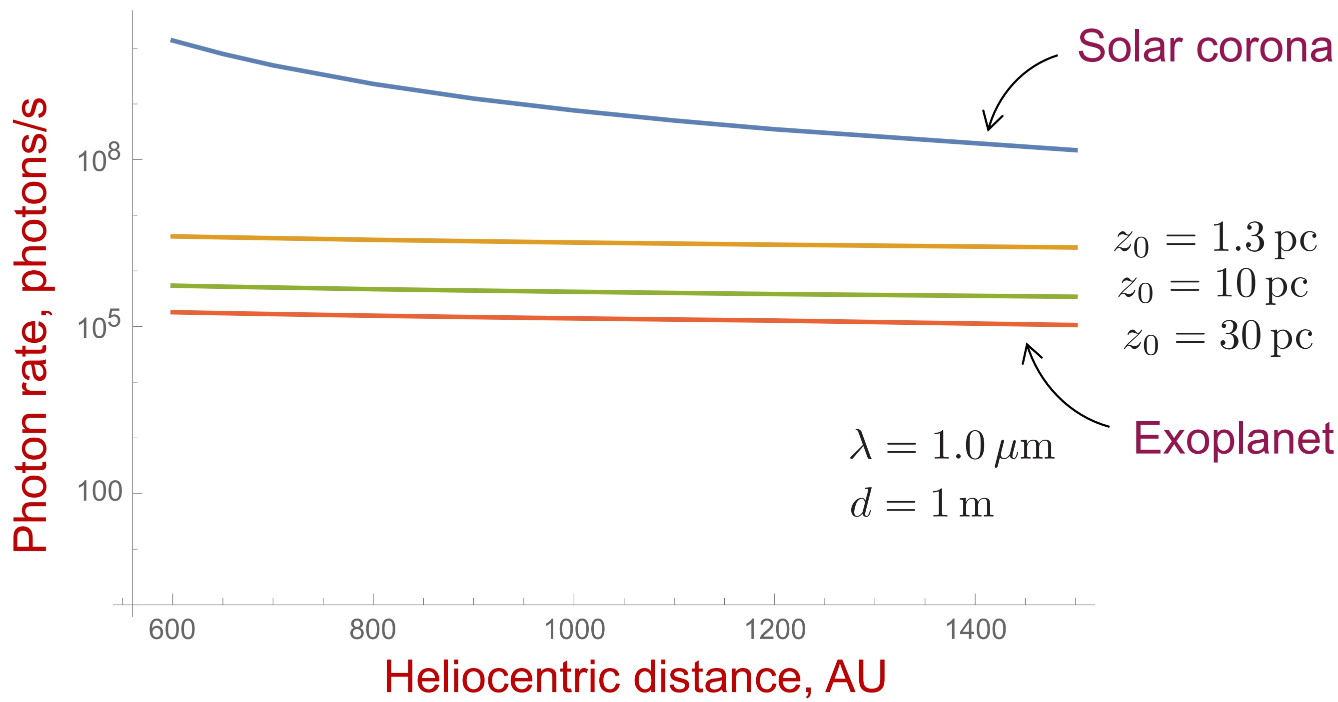

Noise from the solar corona is ~10^3 times stronger than the signal.

SNR for solar gravity lens and corona

Estimating the SNR for the combined system: $$\mathrm{SNR_R} = \frac{\mathrm{Q_{exo}}\sqrt{\tau_1}}{\sqrt{p\mathrm{Q_{cor}}}}$$

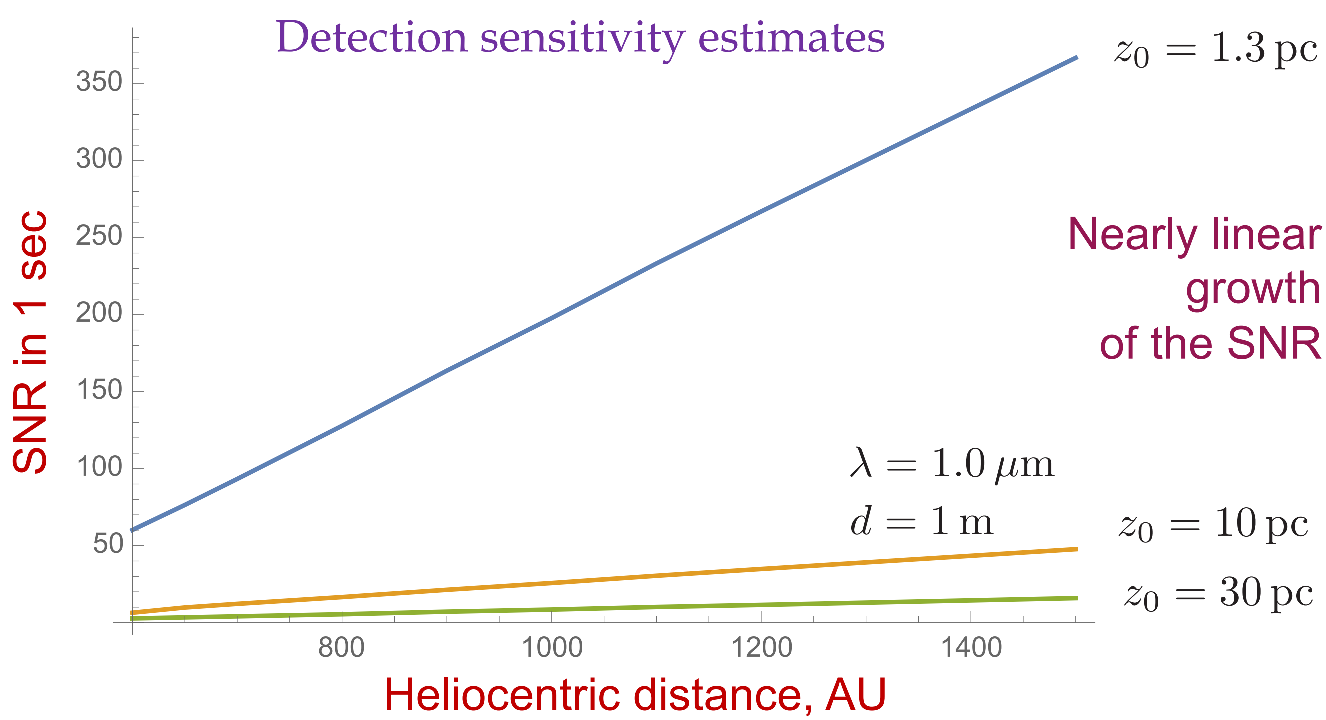

Impact of the solar corona on the detection sensitivity (SNR).

Resolution in 1 and 10 years of integration

Determine number of pixels, N:

$$N = \left(\frac{t_{\mathtt{tot}} \mathrm{Q}^2_{\mathtt{exo}}}{p \mathrm{Q}_{\mathtt{cor}} \mathrm{SNR}^2_{\mathtt{S}}}\right)^{1/4}$$

$t_{\mathrm{tot}} = 1$ year

$t_{\mathrm{tot}} = 10$ years

Number of pixels in 1 year of integration

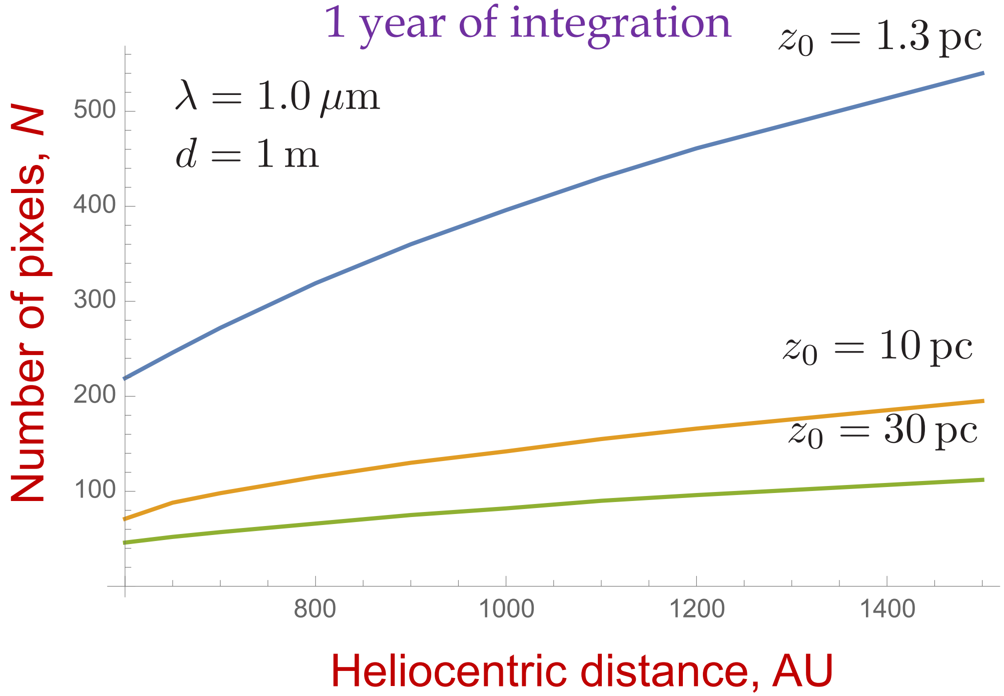

Number of pixels in 10 years of integration

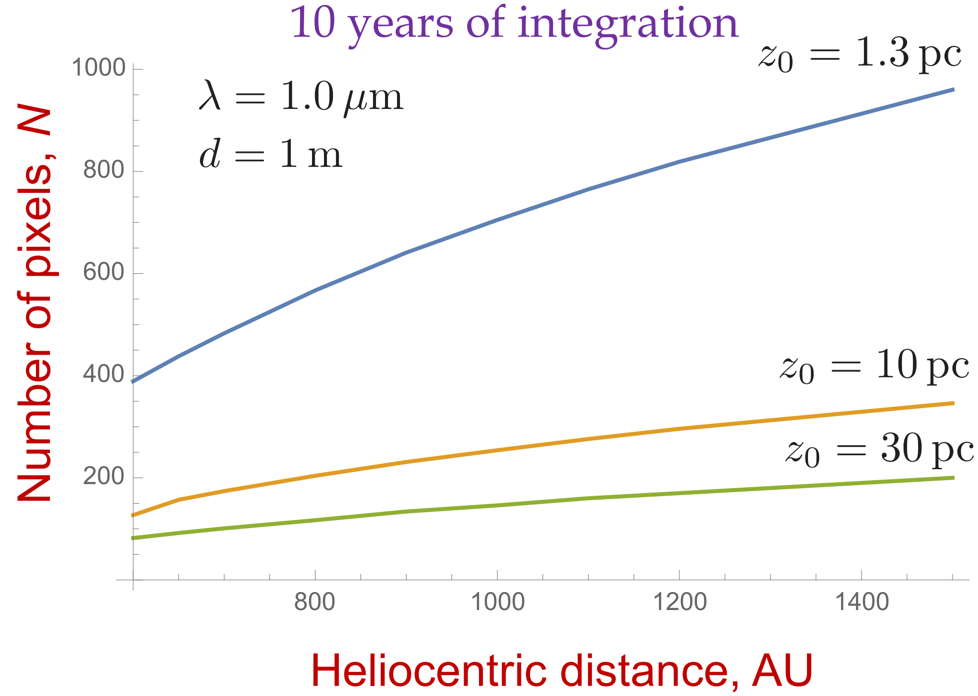

SGL offers pretty impressive capabilities:

To image exo-Earth at 10pc with N = 100 pixels: telescope diameter ~ 3,000 km is needed.

To image exo-Earth at 30pc with N = 100 pixels: telescope diameter ~ 8,850 km is needed.

Achieving High Solar System Exit Velocity

Propulsion Options Considered:

- Chemical: < 15 AU/year
  - Requires large ΔV close to the Sun, and larger SV
- Solar Thermal: 22 AU/year
  - Needs 2-3$R_{\odot}$ flyby requiring a heat shield of >1,000 kg;
  - JPL/MSFC point design was 500 kg spacecraft with 8,000 kg (dry) propulsion stage;
- Nuclear Electric: 20 AU/year
  - 2-stage 30kW SEP/20 kW reaches 20 AU/yr, but maximum 40 year trip time;
- Electric Sail: 12-23 AU/year
  - 20 tethers, each 10 km length ⇒ 23 AU/yr (P. Januhen)
  - 500 kg to ~12 AU/yr (L. Johnson)

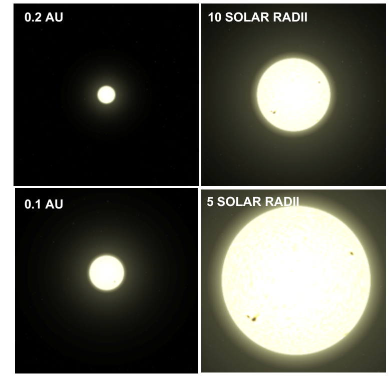

All have features that have high risk, too costly and do not meet desired approach (e.g. share-rides, etc.)

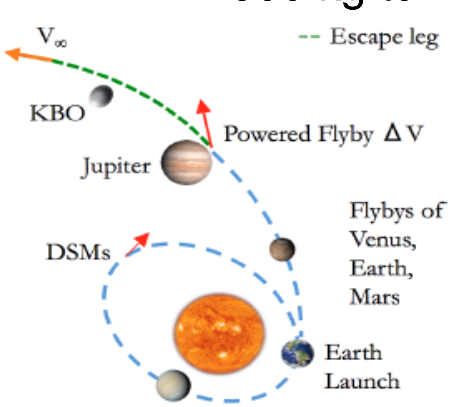

Arora, N., et. al., "Trajectories for a Near Term Mission to the Interstellar Medium"

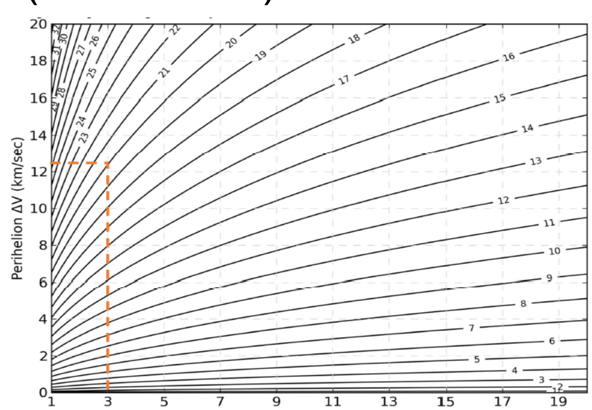

Alkalai, L., et. al., "A Vision for Planetary and Exoplanets Science: Exploration of the Interstellar Medium – The Space Between Stars", 2017

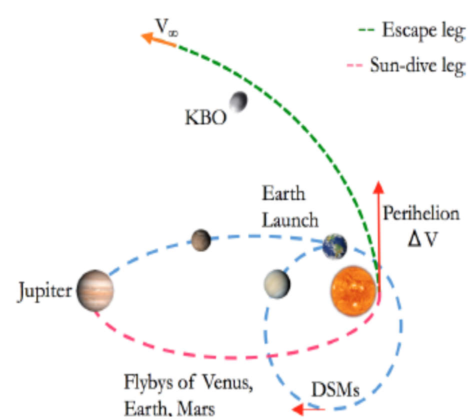

Arora, N., et. al., "Trajectories for a Near Term Mission to the Interstellar Medium"

Baseline Propulsion: Solar Sails for Solar System Exit

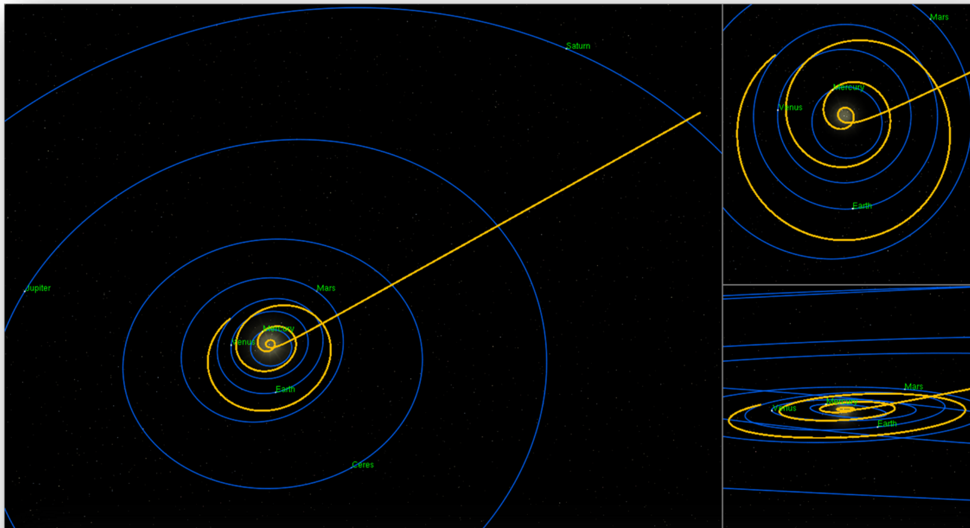

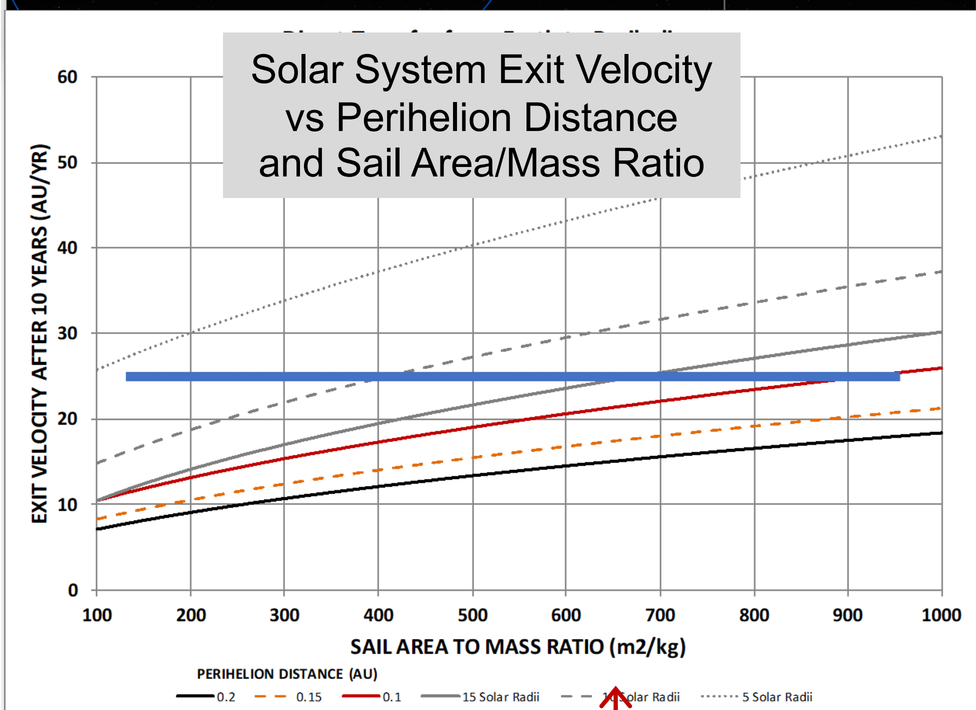

Parker Solar Probe closest approach ~ 9 $R_\odot$

Would like V ~25 AU/yr, to enable a 22 year journey to 550 AU

Solar Sail-driven spiral trajectory controls Perihelion time to match

- exo-star's right ascension and orbit plane Inclination, and
- exo-star's celestial elevation

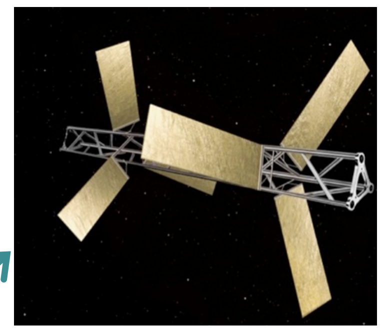

SunVane Sail Design NXTRAC, L·GARDE

- for 10 kg s/c unit, 400 m^2/kg, vane length ~ 100 m

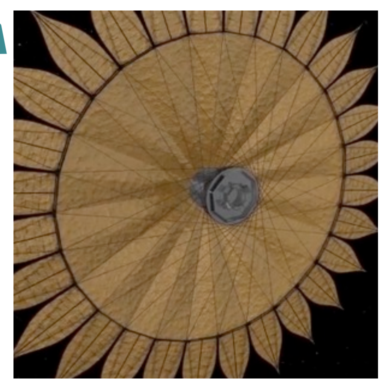

Central portion of the JPL Starshade (not as a coronagraph)

- for 10 kg s/c unit, 400 m^2/kg, dia of sharshade ~ 71m

Current Sails

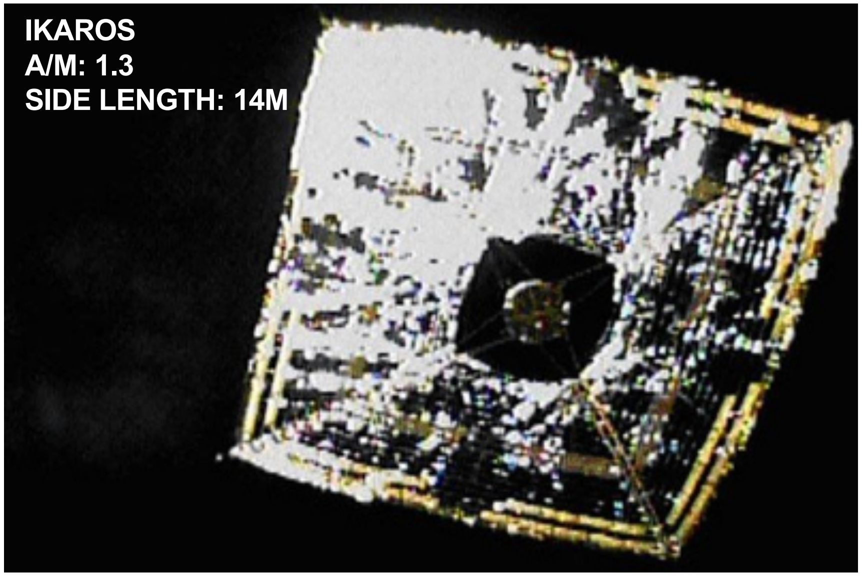

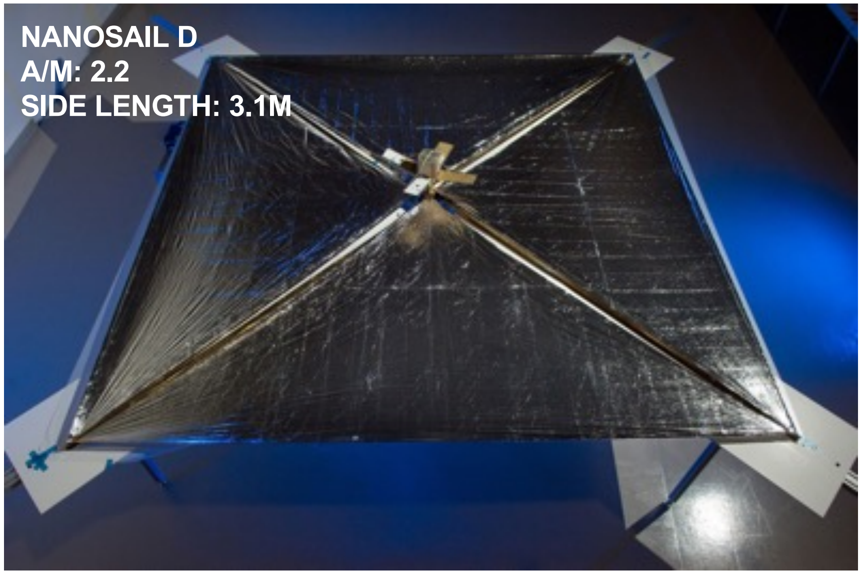

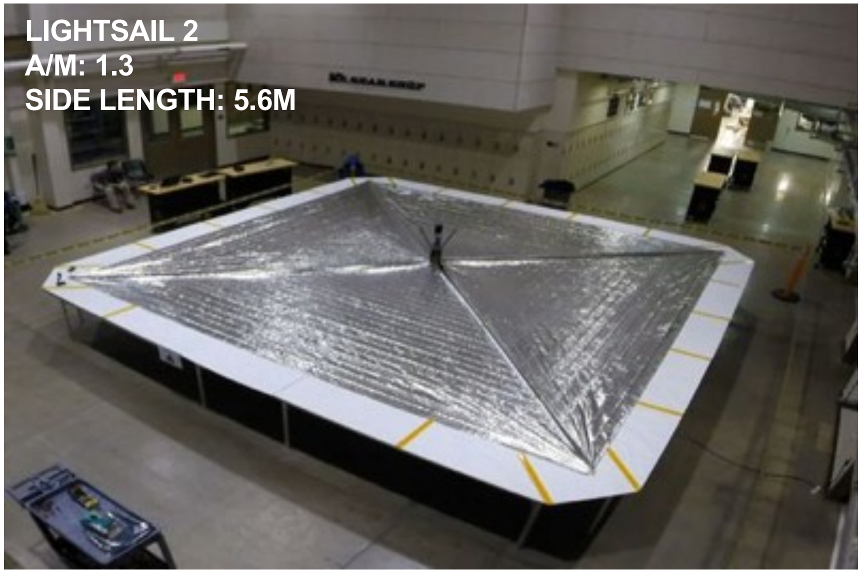

SunVane: A Scalable Approach to Sail Architectures

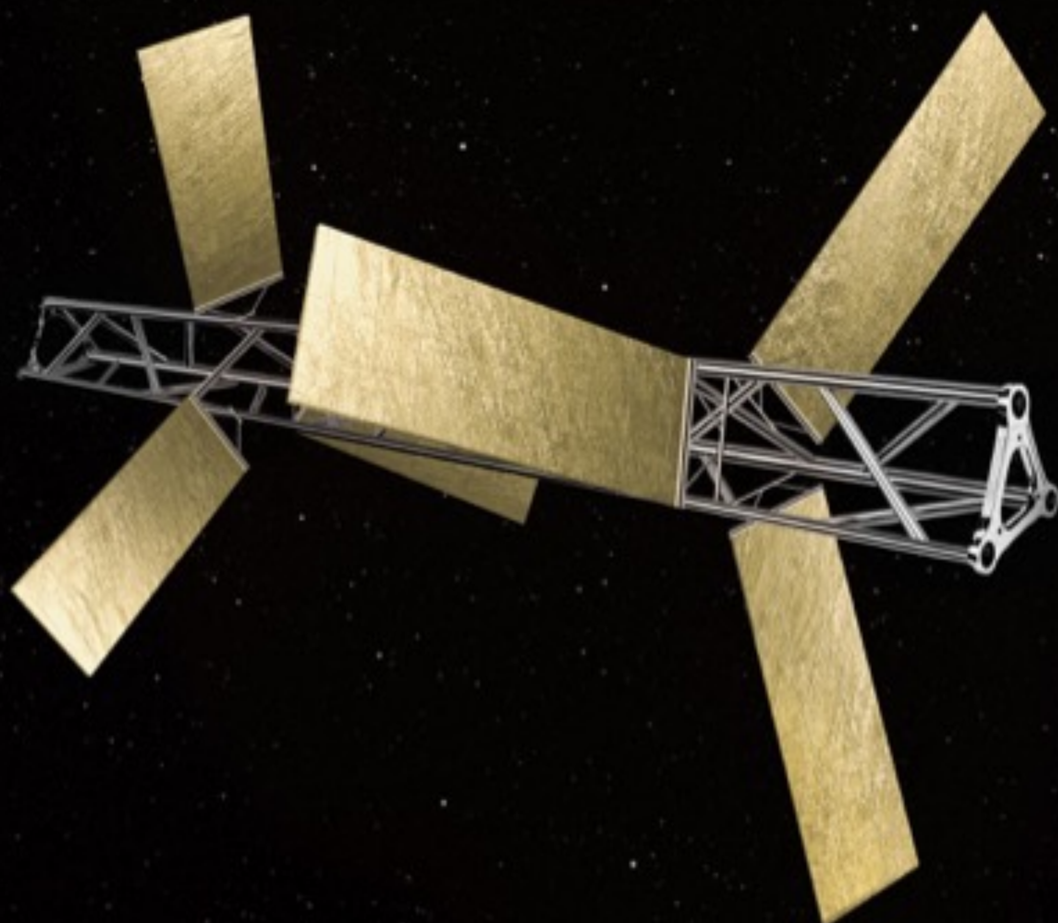

- SIMPLIFIED DEPLOYMENT
- ARTICULATED VANES ENABLE CONTROL
- SIGNIFICANT POWER GENERATION
- SCALES TO 400 A/M RATIO WITH CURRENT TECHNOLOGY
- LEVERAGES TRUSS ADVANCES (< 10 g/m)
- VANES PROVIDE MULTIFUNCTIONAL CABILITIES FOR COMMUNICATION AND POWER GENERATION

THE SOLAR GRAVITATIONAL LENS

Mission CONOPS in Overview

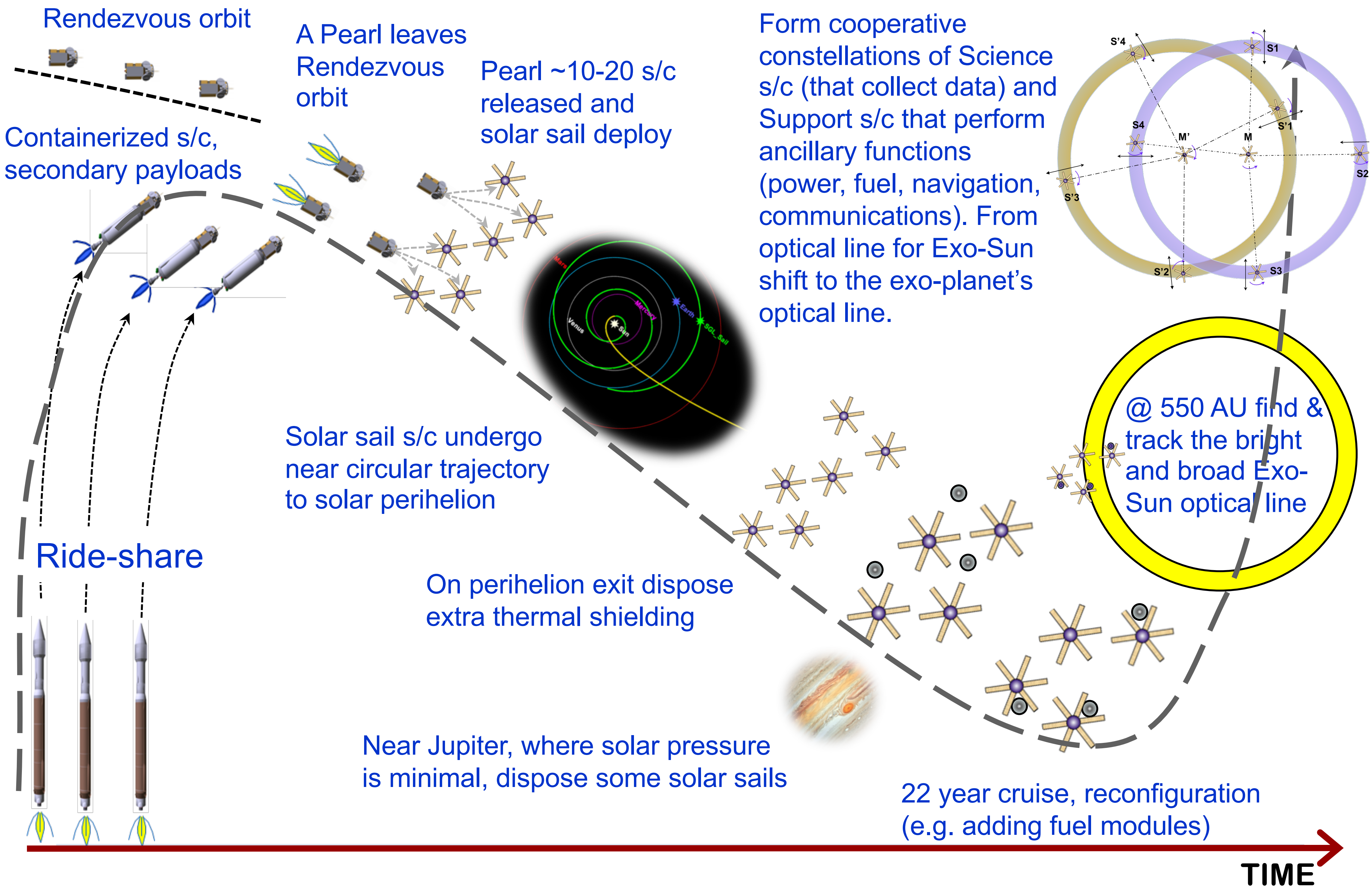

Conclusions

- The knowledge of the physical properties of the SGL much evolved
  - Analytical models for SGL magnification for extended sources
  - Models confirmed with numerical simulations
  - Solar corona is now fully accounted for in the SNR analysis
  - Studied many scenarios of image reconstruction with the SGL
- Improved set of mission-relevant parameters
  - Detection sensitivity; Instrument size and performance; Per pixel integration time;
  - Duration of imaging mission phase; Number of spacecraft; Navigational precision;
  - Formulated mission requirements to deliver a spacecraft beyond 700 AU, to form an imaging system that could exploit the unique optical properties of the SGL.
- Investigated several possible mission architectures
  - Considered: single large s/c, cluster of mid-size s/c, and cluster of solar sail s/c;
  - Baseline architecture: “string of pearls”, based on solar sail propulsion
  - CONOPS for s/c at the SGL to detect, track, and study the Einstein ring
  - Developed a Technology Roadmap and a set of flight demonstrations
- Summary
  - No major showstoppers have been identified
  - Imaging with the SGL is challenging, but feasible

SGL may yield an image an exo-Earth

Image of Our Earth in Physical Colors